Configurational splitting of the giant dipole resonance in nuclei of the 2*s*–2*d* shell

B. S. Ishkhanov, I. M. Kapitonov, and V. G. Neudachin

Scientific-Research Institute of Nuclear Physics, Moscow State University

R. A. Éramzhyan

Institute of Nuclear Research, USSR Academy of Sciences, Moscow
Fiz. Elem. Chastits At. Yadra **14**, 286–328 (March–April 1983)

A universal property of dipole resonance in nuclei of the 2*s*–2*d* shell—configurational splitting—is analyzed. This phenomenon consists of the occurrence of two groups of transitions separated in energy and formed by nucleons of different shells. Experiments that make it possible to observe the splitting in photonuclear reactions are described, and the consequences of such splitting in electron-scattering and muon-absorption reactions are discussed.

PACS numbers: 24.30.Cz

INTRODUCTION

In the investigations of the giant dipole resonance in the absorption of γ rays by nuclei during the last 20 years several stages of development can be traced.

In the sixties, the main attention was devoted to the problem of the formation of this resonance on the basis of a microscopic picture of particle–hole (ph) excitations. The basic idea was provided by Wilkinson,[1] namely, that in the simplest single-particle shell model the ph states excited in dipole absorption are concentrated in a comparatively narrow range of energies E_γ with mean value $\overline{E}_\gamma \approx \hbar\omega$, where $\hbar\omega$ is the distance between single-particle levels of different parity in the oscillator potential (or in the Woods–Saxon potential well), the distance being $\hbar\omega \approx 7$–8 MeV in heavy nuclei and $\hbar\omega \approx 12$–15 MeV in light nuclei. The spin–orbit splitting of the single-particle levels has little influence on the position of the resonance, since in $E1$ transitions there is no spin flip, i.e., transitions of the type $(j = l + \frac{1}{2}) \to (j' = l + 1 - \frac{1}{2})$ are suppressed.

This idea of Wilkinson was coupled with another, no less important, which corresponded to transition to the many-particle shell model: The mixing of states by the effective NN interaction forms a *dipole state* as a coherent sum of ph states and shifts it upward in energy[2] (repulsion of the particle and hole). The same result was obtained either by using simply the procedure of *diagonalization* of the interaction matrix of the ph states[3] (Tamm–Dancoff approximation) or by additionally taking into account *vacuum polarization* (or correlation in the ground state by the random-phase methos).[4,5] This last is particularly important if one considers the case of attraction of the particle and hole, when the collective level sinks appreciably compared with the *zeroth approximation* and the *vacuum* is strongly polarized, giving isoscalar 2^+ and 3^- excitations, etc. As a result, it became clear that the microscopic picture was equivalent to the earlier hydrodynamic description of Migdal.[6]

Then came an intense investigation into the fine structure of the giant resonance: the doubling of the maximum, i.e., the doubling of the dipole state for strongly deformed nuclei,[7] the isospin splitting of the giant dipole resonance,[8] the coupling of hole states to phonon excitations[9] or their spreading over the spectrum of the system of valence nucleons,[10] and the influence of friction, i.e., states of the type 2p–2h, on both the excitation spectrum of the nucleus and the photonucleon spectrum.[11] This stage, like the first, was characterized by great successes in understanding the experimental data and in the prediction of new effects. But even today it is not possible to explain theoretically the details of the fine structure of the giant dipole resonance, though an understanding has been achieved of its comparatively gross properties.

Finally, in recent years there has been active study of other high-lying resonances such as $E0$, $E2$, $M2$, and their decay modes.[12,13] For this purpose, α particles, electrons, nucleons, π mesons, etc., are used.

In this review, the main attention will be concentrated on effects manifested in dipole transitions in light nuclei. These questions were already posed at the time when the very foundations of the particle–hole approach were discussed, but they remained in the background for a long time, since a special experimental method was needed. We are referring to *configurational splitting* of the giant dipole resonance in light nuclei ($A < 40$) and the possible generalizations of this phenomenon. Already in the beginning of the sixties we noted[14] that in light nuclei dipole transitions calculated in the zeroth, or diagonal, approximation are characterized by a spread over a wide energy interval, and diagonalization of the ph interaction matrix does not as a result lead to a single dipole state—the large spread is preserved. The reason for this is the important part played by Majorana forces in light nuclei, which have two specific properties. First, the levels of nuclei of the 1*p* shell (and, to a much lesser degree, of the 2*s*–2*d* shell) are strongly split in accordance with the orbital Young Patterns $[f]$.[15] Second, in nuclei of the 1*p* shell a nucleon excited to the 2*s*–2*d* shell is weakly bound to the core of the *p* nucleons, which, irrespective of its internal state, simply appears as a potential well

 0090-4759/83/020119-19$04.40

for the $2s-2d$ nucleon.[16] Much the same occurs for nuclei of the $2s-2d$ shell when a nucleon is excited to the $3p-3f$ shell. This is due to the fact that with increasing quantum numbers nl of the nucleon the matrix elements of the Majorana forces quickly lose their specific exchange nature and decrease.

The upshot is that for nuclei of the p shell the giant resonance is strongly split in accordance with the Young patterns $[f]$ of the hole states,[17] while for nuclei of the $2s-2d$ shell another circumstance, also present in nuclei of the $1p$ shell,[17] comes to the forefront, namely, when a hole state is formed in the $1p$ shell, its energy increases rather rapidly with increasing A.[18,19] As a result, in nuclei with a sufficiently large number of nucleons in the $2s-2d$ shell ($A>20$), the dipole transitions are separated from the closed shell, $1p \to (2s-2d)$, and are shifted upward in energy. This is the origin of the configurational splitting of the giant dipole resonance[14,20-22]; it plays an important part and in some cases is more important than the other splittings mentioned above. This new form of splitting of the giant dipole resonance is expressed in numerous specific properties, which we discuss below. In particular, it becomes particularly large in processes in which $qR \gtrsim 1$ (q is the momentum transfer and R the radius of the nucleus), i.e., in electron scattering (e, e') and muon absorption.

Thus, there intersect here, complementing each other, two fields of investigation—the physics of photonuclear reactions (and inelastic electron scattering) and the physics of intermediate energies (quasielastic knockout $(p, 2p)$ and $(e, e'p)$ processes,[18] and also pickup reactions at intermediate energies[23]). The need to make direct use of data from quasielastic knockout and pickup reactions instead of Wilkinson's schematic picture for light nuclei was pointed out in Refs. 10, 20, and 21. The interesting properties of the energies of hole states in light nuclei that we have mentioned stimulated theoretical studies by the Hartree–Fock method (see, for example, Refs. 22 and 24), these now having a more reliable basis of experimental data.[18,23]

1. DIPOLE RESONANCE IN NUCLEI OF THE 2s–2d SHELL

In discussing the structure of the dipole resonance in nuclei of the $2s-2d$ shell, we shall assume that the lowest 0s and $1p$ shells are closed. The remaining $n=A-16$ nucleons, where A is the mass number, occupy the $2s-2d$ shell. Then the ground state of the nucleus has the configuration

$$0s^4 1p^{12} (2s-2d)^n. \qquad (1)$$

The experimental data, which we shall discuss in detail in the next section, indicate that this approximation corresponds to reality rather well.

In the region of nuclei we are discussing, the dipole resonance is formed from states with the configurations

$$0s^4 1p^{12} (2s-2d)^{n-1} (3p \text{ or } 3f)^1 \qquad (2)$$

and

$$0s^4 1p^{11} (2s-2d)^{n+1}, \qquad (3)$$

if we restrict ourselves to transitions of a nucleon in only the band of $1\hbar\omega$ excitations. The first is associated with excitation of an outer (valence) nucleon and corresponds to transitions that belong to group A in the terminology used in the review of Ref. 17. The second is associated with excitation of a nucleon of the closed $1p$ shell (group B).

As was already demonstrated in Ref. 17, similar configurations arise in nuclei of the $1p$ shell. The residual nucleon–nucleon interaction has mixed them weakly, and they have preserved their individuality. The same effect occurs in the region of nuclei we are discussing, though, as will be shown below, it is not so clearly expressed because the mixing of the configurations is stronger.

In ^{20}Ne and the nearest nuclei, in which filling of the $2d_{5/2}$ shell is just beginning, it is to be expected that the configurational splitting will be manifested most clearly. The $2d_{5/2} \to 3f_{7/2}$ transitons form group A, and the $1p_{3/2} \to 2d_{5/2}$ transitions from group B, the latter being very strong. In the region of ^{24}Mg–^{28}Si, the $2d_{5/2}$ shell is partly filled. Therefore, configurations associated with the $2d_{5/2} \to 3f_{7/2}$ transition play a more important role, and configurations associated with the $1p_{3/2} \to 2d_{5/2}$ transition are weakened because of blocking. Because of this weakening, $1p_{1/2} \to 2d_{3/2}$ transitions become important in the high-energy part of the spectrum.

If we ignore the spreading of the Fermi surface, then in ^{32}S and all the following nuclei the $2d_{5/2}$ shell is already closed, and there are no $1p_{3/2} \to 2d_{5/2}$ transitions. However, this case is not realized in reality, so that besides the $1p_{1/2} \to 2d_{3/2}$ transition there is also $1p_{3/2} \to 2d_{5/2}$. Thus, the nature of the configurational splitting of the nuclei of the $2s-2d$ shell will depend strongly on the region of nuclei under consideration.

To investigate the configurational splitting of the dipole resonance in nuclei of the $2s-2d$ shell, it is necessary to separate it into components due to transitions of a nucleon from the inner $1p$ ($1p_{3/2}$ and $1p_{1/2}$) shell and the outer $2s-2d$ shell. This can be done by measuring the cross section of the photonucleon channel of the splitting with a fixed final state of the formed nucleus, i.e., by measuring the partial cross sections and using spectroscopic information on the corresponding states. Indeed, the low-lying states of the nuclei of the $2s-2d$ shell of positive parity are described in the majority of cases by the configuration $0s^4 1p^{12} (2s-2d)^{n-1}$. These states can be populated by excitation and subsequent escape of a valence nucleon [see the expression (2)]. The escaping nucleon may be either the one that directly absorbed the γ ray or, by virtue of the channel coupling, a nucleon that did not participate in the absorption.

In the general case, the negative-parity states of the final nucleus $A-1$ are described by the superposition of configurations

$$\alpha_1 \mid (2s-2d)^{n-2} J_1 E_1 (3p \text{ or } 3f)^1\rangle + \alpha_2 \mid 1p_{3/2}^{-1} (2s-2d)^n J_2 E_2\rangle + \alpha_3 \mid 1p_{1/2}^{-1} (2s-2d)^n J_2 E_2\rangle. \qquad (4)$$

For the negative-parity levels of nuclei of the $2s-2d$ shell there are no detailed calculations of configuration mixing. When analyzing their structure, it is necessary to rely mainly on experimental data on pickup and quasifree knockout reactions. As follows from such experimental data (see below), a configuration with a hole in the $1p_{1/2}$ shell is weakly spread and, as a rule, is concentrated on one or two levels. For these levels, the coefficient α_3 in (4) is large. Conversely, a configuration with a hole in the $1p_{3/2}$ shell is very strongly spread over a large number of states.

States of the nucleus $A-1$ with a configuration containing a hole in the $1p$ shell can be populated by decay of a resonance whose structure is determined by the same hole configuration, i.e., $0s^4 1p^{11}\,(2s-2d)^{n+1}$. Thus, the nature of the hole excitation of the final nucleus $A-1$ is the trace that enables one to recognize the transitions that formed the given partial cross section.

After summation of the partial cross sections associated with transitions from the $1p$ and $2s-2d$ shells, we obtain the components of the dipole resonance due to transitions from the inner and outer shells. The reliance on pickup or quasifree proton knockout reactions means that we cannot consider the states of the final nucleus $A-1$ which are hole states relative to the excited states of the initial nucleus.

The number of all the states constructed on the configurations (2) and (3) is so large that realistically only a small fraction of them can be included in calculations. Many of them do not participate directly in the absorption of the γ ray but spread the dipole resonance over a certain energy region. This opens up a large number of decay channels to states of a complicated nature in the final nucleus $A-1$. There is a similar influence of configurations corresponding to transitions of a nucleon to the band of $3\hbar\omega$ excitations, etc. A complete description of the excitation and decay of the resonance requires all these factors to be taken into account. The effects of the spreading of the doorway particle–hole states over more complicated states and the emission of particles in each stage of complication of the doorway state are considered at the present time in the framework of the exciton model.[25] The fact that the state structure of the final nucleus $A-1$ can be extracted from experimental data makes it possible to avoid the difficulties of the theory in describing the details of the nuclear structure, particularly if this is due to the $1p$ hole states.

Thus, combination of experimental data on the partial photodistintegration channels of nuclei of the $2s-2d$ shell with experimental data on the structure of the final hole states solves to a large degree the problem of separating the part of the reaction that proceeds without subsequent strong entangling of states.

Now a few words on terminology. The transitions separated in this manner are called particle–hole or semidirect transitions. It must be borne in mind that particle–hole transitions occur above the real ground state, whose structure may be fairly complicated. In theory, one understands by the expression *particle-hole transition* the simplified case when the maximal number of subshells is closed. When discussing the experimental data, we shall use this term in a wider sense. Essentially, we have an intermediate coupling approximation that takes into account all states of particles in the $2s-2d$ shell.

2. SPECTRA OF HOLE STATES OF NUCLEI OF THE 2s-2d SHELL

We begin the analysis of the structure of the states of nuclei of the $2s-2d$ shell with the nucleus ^{28}Si. The corresponding results of measurements are given in Fig. 1.

Figure 1a shows the energy spectrum of the protons obtained in the ^{28}Si$(e,e'p)$ reaction[26] as a function of the excitation energy of the final nucleus. In the region below 10 MeV, two groups of unresolved levels are observed; they are denoted by $d+s$ and $d+p$ in the figure, and their quantum numbers are determined from the shape of the momentum distributions of the protons. The region of energies above 10 MeV can be divided into two parts (10–30 and more than 30 MeV), in which hole excitations in the $1p$ and $0s$ shells are predominant. In Fig. 1b, the lines give spectroscopic information from proton pickup reactions.[19,27-30] It can be seen that in the region of excitation energies up to 10 MeV the results of the two types of experiment do not contradict each other, though the proton pickup reactions give more accurate information, since the high energy resolution in such experiments makes it possible to investigate individual levels. Therefore, in many cases it is possible in the proton pickup reactions (in contrast to the quasielastic knockout reactions) to determine not only the orbital angular momentum l of the captured proton but also its total angular momentum j.

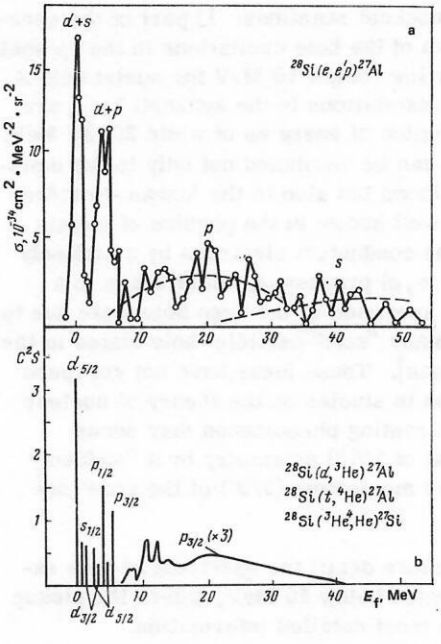

FIG. 1. Comparison of data on proton quasielastic knockout and pickup reactions for the ^{28}Si nucleus.

In the region above 10 MeV, where deep hole excitations ($1p_{3/2}^{-1}$ and $0s_{1/2}^{-1}$) are situated, the pickup reactions are much less informative because of the strong decrease in the effective cross sections due to absorption and growth of the level density. Therefore, there are virtually no corresponding experimental data on pickup. The region above 10 MeV is much better studied in proton quasielastic knockout reactions, which make it possible to determine the centroids and the extent of the spreading of the deep hole excitations.

The paper of Ref. 31 makes it possible to compare the results of quasielastic knockout and pickup experiments for nuclei of the $2s-2d$ shell in the region of excitation energies 10–40 MeV in the final nucleus. It contains a study of the neutron pickup reaction ^{28}Si(^{3}He, α)^{27}Si. The spectrum of neutron hole states of the nucleus ^{28}Si in the region 10–40 MeV, which is no longer a set of resolved levels, is shown by the continuous curve in Fig. 1b (the vertical scale is increased by three times).

In the region below 10 MeV, the information given in Ref. 31 hardly differs from the information that is obtained from the proton pickup reaction (the lines). The possibility of using data on the ^{28}Si(^{3}He, α)^{27}Si reaction to obtain information about proton hole states is based on the fact that proton and neutron pickup in the case of the ^{28}Si nucleus lead to the formation of the mirror nuclei ^{27}Al and ^{27}Si. It can be seen from Fig. 1 that the spectrum of hole excitations in pickup in the region 10–40 MeV has the same nature as in quasielastic knockout. The analysis of the angular distributions and cross sections made in Ref. 31 shows that the discussed section of the spectrum is due to pickup of a nucleon from the $1p_{3/2}$ subshell.

The features of the spectrum of hole excitations observed in the ^{28}Si nucleus are typical of nuclei of the $2s-2d$ shell. We mention two important circumstances that follow from analysis of pickup reactions and nucleon quasielastic knockout reactions: 1) part of the spectroscopic strength of the hole excitations in the $1p$ shell is situated rather low (below 10 MeV for nuclei with $A \leq 32$); 2) the hole excitations in the subshell $1p_{3/2}$ are distributed in a region of energies of width 20–30 MeV. This phenomenon can be attributed not only to the emission of Auger nucleons but also to the Mahan–Nozières effect,[32] which is well known in the physics of metals [polarization of the conduction electrons by a suddenly appearing hole in (γ, e) processes, which leads to a broadening of the spectrum of the deep hole state due to the excitation of many "soft" particle–hole states in the conduction electrons]. These ideas have not yet found adequate reflection in studies on the theory of nuclear reactions. An interesting phenomenon may occur here—the breaking of $SU(3)$ symmetry by a "suddenly appearing" angular momentum $(3/2^-)$ of the core (see below).

We consider in more detail the spectrum of hole excitations in the region below 10 MeV, where the pickup reactions give the most detailed information.

The data obtained in the pickup reactions for nuclei of the $2s-2d$ shell are given in Refs. 23 and 33. We

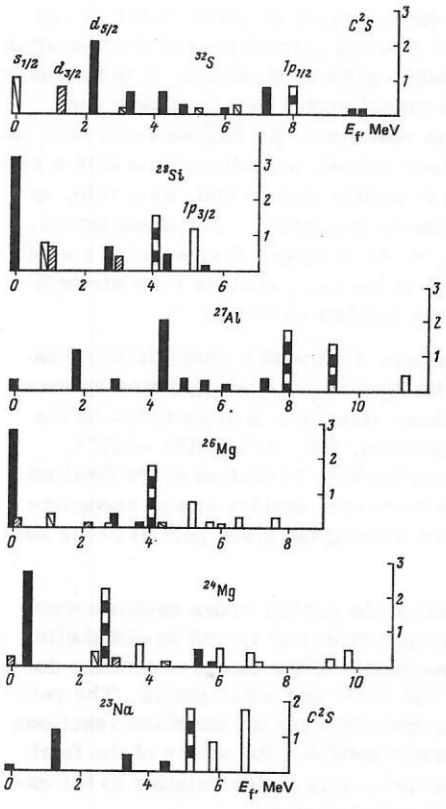

FIG. 2. Spectroscopic characteristics of proton hole states of the nuclei ^{23}Na, ^{24,26}Mg, ^{27}Al, ^{28}Si, and ^{32}S obtained in proton pickup reactions.

shall discuss proton pickup reactions for the nuclei ^{23}Na, ^{24}Mg, ^{26}Mg, ^{27}Al, ^{28}Si, and ^{32}S, since below we analyze the results of the proton decay channel of the giant dipole resonance of these nuclei.

Data on the $(d, {}^3\mathrm{He})$ and $(t, {}^4\mathrm{He})$ proton pickup reactions for the nuclei ^{23}Na, ^{24}Mg, ^{26}Mg, ^{27}Al, ^{28}Si, and ^{32}S are given in Fig. 2, from which one can see the distribution of the proton hole excitations of these nuclei among the levels of the nuclei ^{22}Ne, ^{23}Na, ^{25}Na, ^{26}Mg, ^{27}Al, and ^{31}P. The number of protons in these nuclei is smaller by one. We recall that the spectroscopic factors S of states with definite quantum numbers n, l, and j must satisfy the sum rule

$$\sum C^2S = \langle p \rangle_{n\,lj}, \tag{5}$$

where $C^2 = 2T/(2T+1)$ (T is the isospin of the final nucleus), $\langle p \rangle_{nlj}$ is the number of protons in the nlj subshell, and the summation is over all states of the final nucleus that can be excited following proton pickup from this subshell. Independent information about the number of nucleons in the outer shell is provided by stripping reactions, since the sum rule for the spectroscopic factors of the levels excited in these reactions is directly related to the number of vacancies (holes) in the nlj subshell. For the considered nuclei (^{23}Na, ^{24}Mg, ^{26}Mg, ^{27}Al, ^{28}Si, and ^{32}S) the data on the proton pickup and stripping reactions[23,33] for the numbers of protons in the $2d_{5/2}$, $2s_{1/2}$, and $2d_{3/2}$ subshells agree to within the errors of the experiments. The numbers $\langle p \rangle_{nlj}$ obtained by joint analysis of these two types of experiment

TABLE I. Numbers of protons in different subshells for the corresponding nuclei obtained from proton pickup and stripping[23,33] and theoretical calculations.[24,34,35]

Nucleus		$1p_{3/2}$	$1p_{1/2}$	$2d_{5/2}$	$2s_{1/2}$	$2d_{3/2}$	$2s-2d$
^{23}Na	Experiment	2.4	1.7	2.9	0.1	0	3
	Theory	4	2	—	—	—	
^{24}Mg	Experiment	2.2—2.8	2.2	3.2	0.3	0.5	4
	Theory[34]	4	2	2.86	0.55	0.59	
^{26}Mg	Experiment	1.5—1.8	1.8	3.3	0.5	0.2	4
	Theory[24]	4	2	2.91	0.86	0.23	
^{27}Al	Experiment	0.5—1.0	2.6	4.8	0.2	0	5
	Theory	4	2	—	—	—	
^{28}Si	Experiment	1.2	1.5	4.5	0.75	0.75	6
	Theory[34,24]	4	2	4.48 4.4	0.82 0.7	0.70 0.9	
^{32}S	Experiment	0	0.8	5.75	1.45	0.8	8
	Theory[34,35]	4	2	5.08 5.68	1.51 1.55	1.41 0.77	

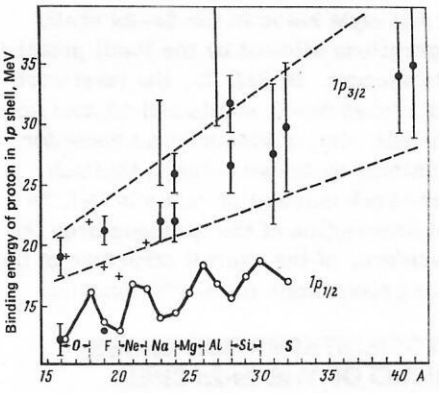

FIG. 3. Binding energies of protons in $1p_{1/2}$ and $1p_{3/2}$ subshells obtained from pickup reactions (open circles) and quasielastic knockout reactions (black circles and vertical lines). The pluses are the binding energies of protons in the $1p_{3/2}$ subshell for nuclei at the start of the $2s-2d$ shell obtained from pickup reactions.

are given in Table I. For the outer subshells, the error of the data given in the table does not exceed 10–20% in the majority of cases.

The spectroscopic information for nuclei of the $2s-2d$ shell has a number of general features:

1) the hole levels in the $2s-2d$ shell are situated mainly in the region of excitation energies 0–8 MeV and exhaust most of the sum rule for this shell;

2) the spectroscopic strength of the hole excitation in the $1p_{1/2}$ subshell is concentrated on one or two states;

3) an appreciable fraction of the spectroscopic strength (40–100%) of the hole excitation in the $1p_{3/2}$ subshell cannot be seen because of the limitation in energy in pickup reactions (Table I).

We can also mention the following. In some cases (^{24,26}Mg, ^{28}Si) the hole excitation in the $1p_{1/2}$ subshell is situated very low in the energy scale (2.6–4.0 MeV). The results of analysis of the pickup reaction given in Fig. 2 as well as of the proton quasielastic knockout reaction indicate a strong spreading of the hole excitation in the $1p_{3/2}$ subshell. This is clearly manifested for the nuclei ^{24}Mg and ^{26}Mg. One observes a general tendency for an increase in the energy of hole excitations in the $1p$ shell with increasing mass number A. For nuclei heavier than ^{32}S, hole excitations in this shell are not seen at all in proton pickup reactions. Among the hole states in the $2s-2d$ shell, the $2d_{5/2}^{-1}$ state is most strongly spread.

Joint analysis of proton pickup and quasielastic knockout reactions makes it possible to determine the binding energy of protons in the $1p_{1/2}$ and $1p_{3/2}$ subshells. The pickup reactions give the most accurate information about the $1p_{1/2}$ subshell, the removal of a proton from this shell leading to the appearance of one or two states at a comparatively low excitation energy ($\lesssim$10 MeV). In this energy region, the quasielastic knockout reactions cannot, because of the low energy resolution, distinguish the $1p_{1/2}^{-1}$ state from the strong background of states excited by stripping of a proton from the $2s-2d$ shell. In contrast, data on the low-lying $1p_{3/2}$ subshell with strong energy spreading must be taken from quasielastic knockout reactions. The $1p^{-1}$ state observed in the spectrum of these reactions, which reaches a width of about 20–30 MeV, corresponds to proton stripping from the $1p_{3/2}$ subshell.

Data on the binding energies of protons in the $1p_{1/2}$ and $1p_{3/2}$ subshells for nuclei with $16 \leq A \leq 40$ and taken from pickup[23,33] and quasielastic knockout[18] reactions are given in Fig. 3. For nuclei at the beginning of the $2s-2d$ shell, information about the $1p_{1/2}$ and $1p_{3/2}$ subshells can be obtained from experiments of both types. Thus, for ^{16}O and ^{19}F, quasielastic knockout reactions give the position of the hole excitations in the $1p_{1/2}$ subshell. For ^{16,18}O, ^{19}F, ^{20,22}Ne, the pickup reactions make it possible to find the centroids of the $1p_{3/2}^{-1}$ excitations, since the states observed in these reactions exhaust not less than 80% of the sum rule for the $1p_{3/2}$ subshell. Figure 3 shows where a direct comparison is possible, i.e., for nuclei at the beginning of the $2s-2d$ shell, the pickup and quasielastic knockout reactions give consistent results.

The data given in Table I also characterize the structure of the valence shells of the considered nuclei. It follows from the table that the ground states of the nuclei ^{24,26}Mg, ^{28}Si, and ^{32}S do not correspond to maximal population of the lowest subshells ($2d_{5/2}$ for ^{24,26}Mg, ^{28}Si; $2d_{5/2}$ and $2s_{1/2}$ for ^{32}S), i.e., there is intermediate coupling and the admixture of higher subshells is fairly large, of order 10–30%.

The calculations in the framework of the many-particle shell model[24,34,35] give numbers of protons in the $2d_{5/2}$, $2s_{1/2}$, and $2d_{5/2}$ subshells close to the experimental numbers (see Table I). In Ref. 34, the nuclei ^{24}Mg and ^{28}Si were regarded as made up of the inert core of ^{16}O and valence nucleons in the $2s-2d$ shell. The nucleus ^{32}S was regarded as being made up of the

inert core of ^{40}Ca and eight holes in the $2s-2d$ shell. All possible configurations allowed by the Pauli principle were taken into account. In Ref. 35, the inert core for ^{32}S consisted of closed $0s-1p$ shells and 10 nucleons from the $2d_{5/2}$ subshell, i.e., allowance was made for configurations containing up to two holes in this subshell. The Hartree–Fock calculation made in Ref. 24 gives a fairly good description of the nucleons over the subshells and, therefore, of the overall structure of the wave function of the ground state of the ^{28}Si nucleus.

3. PARTIAL PHOTODISINTEGRATION CROSS SECTIONS OF NUCLEI OF THE 2s-2d SHELL

Below, we shall give experimental data for the photoproton decay channel of the giant dipole resonance of nuclei of the $2s-2d$ shell. This is the predominant channel for the majority of stable nuclei of this region.

The partial cross sections of the photoproton reaction for the nuclei ^{23}Na, ^{24}Mg, ^{26}Mg, ^{17}Al, ^{28}Si, and ^{32}S obtained from photoproton spectra are given in Refs. 36–41. For comparison with the results of proton pickup reactions, it is convenient to use the distribution of the intensity of transitions to different states of the final nucleus $A-1$ in the (γ,p) reaction (the procedure for obtaining such distributions from the photoproton spectra is described in Ref. 17). These distributions for the nuclei ^{24}Mg, ^{27}Al, and ^{28}Si are compared in Fig. 4 with the spectroscopic factors determined in the proton pickup reaction. It can be seen that the position of the maxima in the distributions of the transition intensity in the (γ,p) reaction is correlated with the position of the levels of the nucleus $A-1$ that have large spectroscopic factors in the proton pickup reactions. This permits the conclusion that the giant dipole resonance of nuclei of the $2s-2d$ shell is to a large degree formed by particle–hole excitations. Thus, for the even–even nuclei ^{24}Mg and ^{28}Si between 60 and 80% of the integrated cross section of the (γ,p) reaction is concentrated on them.[38,40]

Similar conclusions are reached by the investigation of the spectra of γ rays that carry away the excitation of the final nuclei formed in photonucleon reactions, i.e., the $(\gamma,p\gamma')$ and $(\gamma,n\gamma')$ processes. We analyzed the experimental data for nuclei of the $2s-2d$ shell.[42-50] In all cases (we investigated the nuclei ^{16,18}O, ^{19}F, ^{23}Na, ^{24,25,26}Mg, ^{28}Si, ^{32}S, and ^{40}Ca) not less than 90% of the decays were to levels of the final nucleus revealed in the nucleon pickup reactions.

The partial cross sections extracted from the photonucleon spectra can usually be formed by population of a group of states of the final nucleus, since the resolution with respect to the energy of the final nucleus for such partial cross sections is usually 1 MeV. However, not all these states are populated with significant probability. The data on the spectra of the γ rays that carry away the excitation of the final nuclei, and the clear correlation with pickup, make it possible to determine what states are populated, and with what probability, in the region of excitation energies of the final nucleus up to 5–6 MeV. The interpretation of the partial cross sections for population of states with energies higher than 5–6 MeV in the final nucleus is not so unambiguous, since for this energy region there are usually no data on the spectra of γ rays.

We consider as an example the ^{27}Al$(\gamma,p)^{26}$Mg reaction.[36] For this reaction, the cross sections were obtained for population of the ground state and the first and second excited states of the final nucleus (1.81 and 2.94 MeV), and also groups of states whose centroids $\overline{E}_f$ are situated at the energies $\overline{E}_f = 4.4$, 6.6, 8.5, 11.0, and 13.0 MeV. The analysis of the partial cross sections was based on comparison with data on the proton pickup reactions ^{27}Al$(d,^3$He$)^{26}$Mg (Refs. 51–53; Fig. 5) and ^{27}Al$(n,d)^{26}$Mg.[54]

It can be seen from Fig. 5 that the first five partial cross sections ($\overline{E}_f = 0, 1.8, 2.9, 4.4, 6.6$ MeV) are formed by transitions from the $2d_{5/2}$ subshell. Transitions from the $1p$ shell make a contribution to the remaining partial cross sections ($\overline{E}_f = 8.5$, 11.0, and 13.0 MeV). There is good correlation between the pickup-reaction data and the results of the (γ,p) experiment. The states of the final nucleus whose population cross sections in the (γ,p) reaction have the largest values also correspond to the largest values of the spectroscopic fac-

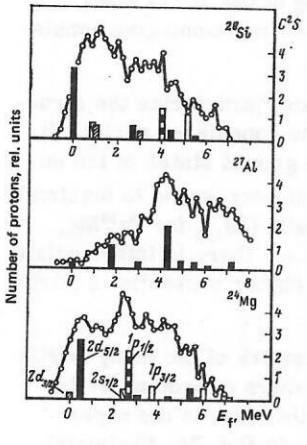

FIG. 4. Comparison of the intensity distributions of transitions to different states of the final nucleus in the (γ,p) reaction (continuous curves) and spectroscopic factors of proton pickup reactions (columns) for the nuclei ^{24}Mg, ^{27}Al, and ^{28}Si.

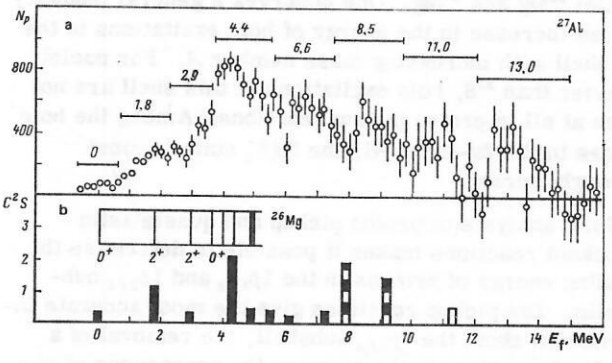

FIG. 5. Intensity of population of different states of the final nucleus (a) in the ^{27}Al$(\gamma,p)^{26}$Mg reaction[36] and spectroscopic factors (b) in the proton pickup reaction.[51-54] Figure 5b also shows the level scheme of the final nucleus ^{24}Mg.

TABLE II. Comparison of relative spectroscopic factors $(C^2S)_{rel} = \sum C^2S/\langle p \rangle$ of proton pickup and integrated values $\sigma_f^{int} = \int_0^{30} \sigma_f(E_\gamma) dE_\gamma$ of the partial cross sections of the (γ, p) reaction for the ^{27}Al nucleus.

Energy E_f of the final ^{26}Mg nucleus, MeV	Shell from which the proton is removed	$(C^2S)_{rel}$, %	σ_f^{int}, %
0	$2s-2d$	6	6
1.81	$2s-2d$	18	18
2.94	$2s-2d$	4	15
4.4	$2s-2d$	46	40
6.6	$2s-2d$	16	20
8.5	$1p$	43	46
11.0	$1p$	8	31
13.0	$1p$	—	23

tors. This is a good illustration of the conclusion that the states of the giant resonance of the ^{27}Al nucleus have an appreciable particle–hole component. In Table II, we compare the relative partial cross sections of the (γ, p) reaction with the relative total spectroscopic factors, which were calculated as $(C^2S)_{rel} = \sum C^2S/\langle p \rangle$, where the summation was over all states of the final nucleus that could contribute to the given partial cross section, and $\langle p \rangle$ is the number of protons in the $2s-2d$ or $1p$ shells. The comparison was made separately for the first five partial cross sections, which are due to transitions from the outer shell, and for the last three cross sections, to which transitions from the inner shell contribute.

It follows from Table II that for states of the final nucleus with $\overline{E}_f = 0$, 1.8, 4.4, 6.6, and 8.5 MeV the relative values of the spectroscopic factors and the relative cross sections of the (γ, p) reaction are practically equal. It can be concluded from this that the (γ, p) transitions associated with these levels take place mainly because of the decay of particle–hole configurations. About 60% of the integrated cross section of the ^{27}Al$(\gamma, p)^{26}$Mg reaction is associated with these partial transitions.

The sum of the first five partial cross sections ($\overline{E}_f = 0$–6.6 MeV) forms the cross section of the transitions from the outer shell. It is shown in Fig. 6a. Transitions from the inner shell contribute to the remaining partial cross sections ($\overline{E}_f = 8.5$, 11.0, and 13.0 MeV). The sum of these partial cross sections is shown in Fig. 6b. It should be noted that the precise contribution of the transitions from the inner shell to the partial cross sections for population of the states with $\overline{E}_f = 11.0$ and 13.0 MeV is not known, since these cross sections are to a considerable degree formed by decay of configurations more complicated than particle–hole configurations, as is indicated by the absence of correlation between the values of the spectroscopic factors and the integrated cross sections for the population of these states (see Table II). The cross section for population of the states with $\overline{E}_f = 8.5$ MeV is a quite definite part of the cross section of transitions from the inner shell. It

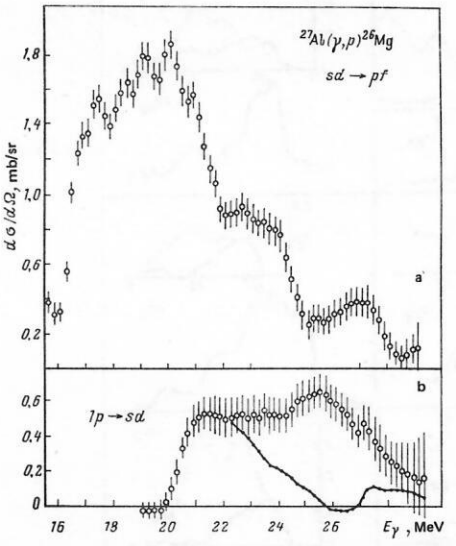

FIG. 6. Sum of partial cross sections of the ^{27}Al$(\gamma, p)^{26}$Mg reaction with formation of the final nucleus in states with $E_f = 0$–6.6 MeV (a) and $E_f > 6.6$ MeV (b). The continuous curve shows the partial cross section for population of states of the final nucleus with $\overline{E}_f = 8.5$ MeV.

is almost entirely formed by transitions from the $1p_{1/2}$ subshell.

The cross sections given in Fig. 6 make it possible to estimate the configurational splitting (the difference between the centroids of the transitions from the inner and outer shells) and the probability of the transitions from the outer shell. The configurational splitting of the ^{27}Al nucleus is obtained as the difference between the centroids of the cross sections shown in Figs. 6a and 6b, and it lies in the range 2.8–4.0 MeV, the smaller value corresponding to the case when the partial cross section for population of the states with $\overline{E}_f = 8.5$ MeV is taken as the cross section of the transitions from the inner shell. A more probable value (but not yet the upper bound) of the configurational splitting (4.0 MeV) corresponds to the assumption that the partial cross sections for population of the states with $\overline{E}_f = 11.0$ and 13.0 MeV are formed mainly by transitions from the inner shell. It is natural to suppose that these higher-lying excitations are also associated with a $1p_{3/2}^{-1}$ hole, which, as we have noted above, induces many-particle "soft" excitations within the configuration $(2s-2d)^n$.

The probability of transitions from the outer shell is in the interval 0.74–0.87. The spread in the estimate is due to the current uncertainty in the interpretation of the partial cross sections for population of high-lying states of the final nucleus ^{26}Mg ($\overline{E}_f = 11.0$ and 13.0 MeV). The results of photoproton experiments on other nuclei of the $2s-2d$ shell, namely, ^{23}Na, ^{24}Mg, ^{26}Mg, ^{28}Si, ^{32}S, were analyzed similarly.[37-41] In all cases, we separated a cross section of transitions from the outer shell formed mainly by the decay of particle–hole configurations and a guaranteed part of the cross section of transitions from the inner shell, due mainly to the decay of the $1p_{1/2}^{-1}(2s-2d)$ component of this cross section.

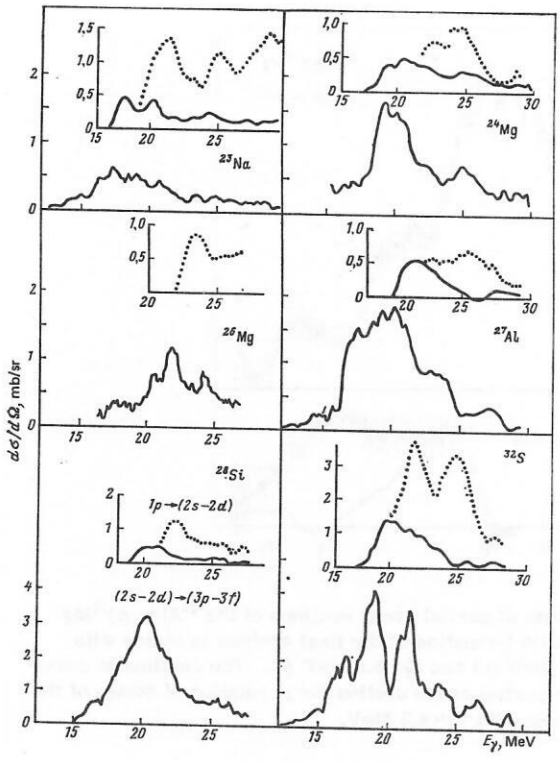

FIG. 7. Results of decomposition of the photoproton reaction cross sections for the nuclei ^{23}Na, ^{24}Mg, ^{26}Mg, ^{27}Al, ^{28}Si, and ^{32}S into components due to transitions from the $2s-2d$ and $1p$ shells. In the inserts, the continuous curves show the cross sections of transitions from the $1p_{1/2}$ subshell (for ^{26}Mg, not determined; for ^{32}S an upper bound is given), and the dotted curves are upper bounds on the cross sections of transitions from the $1p$ shell, i.e., with allowance for transitions from the $1p_{3/2}$ subshell.

The results of the analysis are given in Fig. 7. For the ^{26}Mg nucleus, the cross section of the $1p_{1/2}\rightarrow(2s-2d)$ transitions is small, and its shape was not determined. Only its centroid (Table III) can be found with sufficient accuracy. For the nucleus ^{32}S, the cross section of the $1p_{1/2}\rightarrow(2s-2d)$ transitions given in Fig. 7 is an upper bound.

TABLE III. Centroids ($\overline{E}$) of the cross sections of different transitions and their differences ($\Delta\overline{E}$) (estimates obtained for the region of excitation energies $\lesssim 30$ MeV.

Nucleus	$(2s-2d)\rightarrow(3p-3f)$ $\overline{E}$, MeV	$1p_{1/2}\rightarrow(2s-2d)$ $\overline{E}$, MeV	$\Delta\overline{E}$, MeV	Nucleus	$(2s-2d)\rightarrow(3p-3f)$ $\overline{E}$, MeV	$1p_{1/2}\rightarrow(2s-2d)$ $\overline{E}$, MeV	$\Delta\overline{E}$, MeV
^{23}Na	20.1	22.0	1.9 (4.2)	^{28}Si	20.9	22.2	1.3 (2.5)
^{24}Mg	21.6	22.8	1.2 (2.0)	^{31}P	21—22	25	3—4
^{26}Mg	22.1	23—24	1—2 (2—3)	^{32}S	20.4	21.9	1.5 (2.9)
^{27}Al	20.4	23.2	2.8 (4.0)	^{40}Ca	20—21	25	4—5

Note. In the brackets in the last column we give the configurational splittings obtained under the assumption that the partial cross sections for population of the highest levels of the final nuclei are formed by transitions from the $1p_{3/2}$ subshell.

4. THE ENERGY POSITION OF TRANSITIONS FROM DIFFERENT SHELLS

Data on the energy position of the $(2s-2d)\rightarrow(3p-3f)$ and $1p_{1/2}\rightarrow(2s-2d)$ transitions are given in Table III. We indicate the centroids ($\overline{E}$) of the corresponding transitions, and also their differences $\Delta\overline{E}$, which characterize the configurational splitting. In Table III, we also give information for two nuclei (^{31}P and ^{40}Ca) for which the separation of the $1p_{1/2}\rightarrow(2s-2d)$ component of the photoproton cross section has not been made experimentally. However, the data available for these nuclei are sufficient to obtain reliable estimates. The shape of the total cross section of the (γ,p) reaction for ^{31}P and ^{40}Ca is known.[55,56] For the ^{40}Ca nucleus, the cross section of transitions from the outer shell up to excitation energy 25 MeV is also known.[56] In addition, it follows from data on the proton pickup reaction[23,33] that excitation energies of the final nuclei (^{30}Si and ^{39}K) not less than 10 MeV correspond to a proton hole in the $1p_{1/2}$ subshell. Thus, only the partial cross sections of the ^{31}P$(\gamma,p)^{30}$Si and ^{40}Ca$(\gamma,p)^{39}$K reactions with formation of the final nuclei in states with $E_t>10$ MeV can contain a contribution of $1p_{1/2}\rightarrow(2s-2d)$ transitions. As follows from the experiments, for nuclei of the $2s-2d$ shell[36-41] the centroids and maxima of such cross sections are situated at energies $\gtrsim 25$ MeV, and their contribution to the integrated cross section of the (γ,p) reaction up to the energy 30 MeV does not exceed 15–20%. Obviously, the maximum of the cross section of the $(2s-2d)\rightarrow(3p-3f)$ transitions for ^{31}P and ^{40}Ca coincides with the maximum of the total photoproton cross section (20 and 19 MeV, respectively).

The possibility of transitions from the inner shell in the doubly magic nucleus ^{40}Ca is due to the fact that the ground state of this nucleus does not correspond to a completely filled $2s-2d$ shell. As follows from the single-nucleon transfer reactions, the $2s-2d$ proton shell is not completely filled in the ground state of the ^{40}Ca nucleus[23,33] and the admixture corresponds to the $3p-3f$ shell. It can be seen from Table III that the centroids of the cross sections of transitions from the outer shell are situated around 20–22 MeV. The centroids of the transitions from the $1p_{1/2}$ subshell are around 22–25 MeV.

The energy splitting of the $1p_{1/2}\rightarrow(2s-2d)$ and $(2s-2d)\rightarrow(3p-3f)$ transitions fluctuates strongly from nucleus to nucleus (see Table III), remaining in the range 1–5 MeV. As we have noted above, the configurational splitting in the nuclei of the $2s$ and $2d$ shell is due to the fact that for these nuclei the separation energy of nucleons in the $1p$ shell exhibits a tendency to increase with increasing mass number, whereas the separation energy of a nucleon in the $2s-2d$ shell remains at approximately the same level. The coupling of these two quantities can be clearly seen in Fig. 8, in which the energy distribution of the $1p_{1/2}\rightarrow(2s-2d)$ and $(2s-2d)\rightarrow(3p-3f)$ transitions is compared with the energy of a proton hole excitation in the $1p_{1/2}$ subshell obtained in the pickup reaction. One observes a clear correlation between the two quantities. Figure 8 also shows the general tendency for the configurational splitting to in-

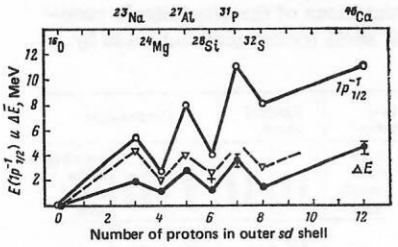

FIG. 8. Comparison of energy splitting of the transitions $1p_{1/2} \rightarrow (2s-2d)$ and $(2s-2d) \rightarrow (3p-3f)$ (black circles) and energies of the proton hole excitation in the $1p_{1/2}$ subshell (open circles); estimate of the configurational splitting with allowance for transitions from the $1p_{3/2}$ subshell (triangles), and the result of calculation of the configurational splitting for the ^{28}Si nucleus (the cross).[40-57]

crease with increasing number of protons in the outer shell, which is also naturally expected from the systematic increase in the binding energy of the $1p$ nucleons with increasing A.

The most reliable estimate of the configurational splitting must take into account transitions from the $1p^{3/2}$ subshell. Transitions from this shell contribute to the partial cross sections for population of the highest levels of the final nuclei. Allowance for the $1p_{3/2} \rightarrow (2s-2d)$ transitions increases the estimate of the configurational splitting deduced from the centroids of the cross sections by about 1–2 MeV (see the numbers in the brackets in the last column of Table III). The configurational splitting of nuclei with odd Z by 1.5–2.0 MeV is greater than for neighboring nuclei with even Z (see the last column of Table III). Thus, the configurational splitting of the giant dipole resonance estimated from the centroids of the cross sections is about 1–3 MeV for nuclei at the beginning of the $2s-2d$ shell and 6–7 MeV for nuclei at the end of the $2s-2d$ shell with an odd number of protons.

It must be emphasized that all the above estimates of the configurational splitting refer to the region of excitation energies up to 30 MeV. It is well known that an appreciable fraction (about 20–30%) of the integrated photodisintegration cross section is situated at $E_\gamma > 30$ MeV. In this region, the importance of transitions from the $1p_{3/2}$ subshell increases. Therefore, the above estimates of the configurational splitting are to be regarded as lower bounds.

Evidence for a predominant contribution of transitions from the $1p_{3/2}$ subshell in the region above 30 MeV is as follows: 1) In all theoretical calculations in which the position of the hole in the $1p_{3/2}$ shell has been correctly chosen the centroid of the $1p_{3/2} \rightarrow (2s-2d)$ transitions is situated at excitation energies 30–40 MeV, and these transitions in the considered region of energies are predominant (see, for example, the calculations of Refs. 10 and 57 for ^{32}S); 2) the strong spreading of the $1p^{-1}_{3/2}$ state (its width is about 20–30 MeV) has the consequence that the $1p_{3/2} \rightarrow (2s-2d)$ transitions will fill the region of energies up to 50 MeV; 3) the relative contribution of the photodisintegration cross section in the region 30–50 MeV agrees with the contribution that must be made to this cross section by the transitions due to the part of the spectroscopic strength of the $1p_{3/2}$ hole that is not touched in excitations with energy less than 30 MeV.

It should be noted that with increasing excitation energy kinematic factors such as the penetrability will favor the decay of the $1p^{-1}_{3/2}(2s-2d)^{n+1}$ configuration with escape of a nucleon to the continuum and formation of the final nucleus in the hole state $1p^{-1}_{3/2}$.

To estimate an upper bound for the configurational splitting, we chose two nuclei—the even–even nucleus ^{28}Si and the odd–even nucleus ^{27}Al, for which the shape of the photoabsorption cross section is well known up to 50 MeV.[58] Under the assumption of a dominant role of the $1p \rightarrow (2s-2d)$ transitions in the region 30–50 MeV and with allowance for the shape of the photoabsorption cross sections in this region we calculated the centroids of the transitions from the $1p$ shell (as the cross sections of the transitions from the $1p$ shell in the region 20–30 MeV we used the dotted curves in Fig. 7). For both nuclei (^{27}Al and ^{28}Si), the centroids of the $1p \rightarrow (2s-2d)$ transitions were at 33–34 MeV. This means that the upper limit of the configurational splitting for these nuclei is 12–14 MeV.

We compare the obtained estimates of the configurational splitting with the isospin splitting ΔE_T (for nuclei with $N \neq Z$). We consider the three nuclei ^{23}Na, ^{27}Al, and ^{31}P, for which the isospin of the ground state is $T_0 = (N-Z)/2 = \frac{1}{2}$. Using the well-known relation $\Delta E_T = 60(T_0+1)/A$ MeV,[59] we obtain an isospin splitting equal to about 3–4 MeV. Thus, the estimates of the configurational splitting obtained in this section indicate that it plays an important part in forming the width (the region of the energy spread) of the giant dipole resonance of nuclei of the $2s-2d$ shell.

5. PROBABILITY OF TRANSITIONS FROM THE OUTER SHELL

The probability of transitions from the outer shell for the nuclei ^{23}Na, ^{24,26}Mg, ^{27}Al, ^{28}Si, and ^{32}S was calculated as the ratio of the integrated photoproton cross sections due to the $(2s-2d) \rightarrow (3p-3f)$ transitions to the total integrated cross section of the (γ, p) reaction.[36-41] The obtained probabilities are given in Table IV, which also contains information on five nuclei of the $2s-2d$ shell: ^{16}O, ^{18}O, ^{19}F, ^{31}P, and ^{40}Ca. For ^{16}O, the information is taken from Ref. 42, which gives the partial cross sections of the (γ, p) reaction and data of a $(\gamma,$

TABLE IV. Probabilities of electric dipole transitions from the outer $2s-2d$ shell obtained from the partial photoproton cross sections.

Nucleus	Probability	Highest photon energy, MeV	Reference	Nucleus	Probability	Highest photon energy, MeV	Reference
^{16}O	0.06—0.11	28.7	[42]	^{27}Al	0.74—0.87	29.7	[36]
^{18}O	0.04—0.12	28.0	[50]	^{28}Si	0.73—0.91	28.0	[40]
^{19}F	0.10—0.18	30.0	[44]	^{31}P	0.7—1.0	30.0	[55]
^{23}Na	0.27—0.56	30.0	[37]	^{32}S	0.51—1.0	29.0	[41]
^{24}Mg	0.65—0.80	30.0	[38]	^{40}Ca	0.8—1.0	30.0	[56]
^{26}Mg	0.66—1.0	27.0	[39]				

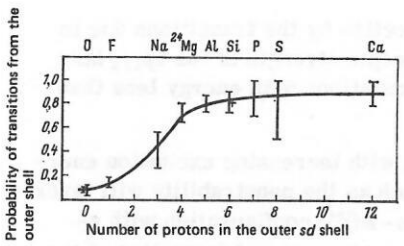

FIG. 9. Probability of $(2s-2d) \rightarrow (3p-3f)$ transitions in the photoproton decay channel of the giant resonance of nuclei of the $2s-2d$ shell. The cross shows the result of a calculation for the ^{28}Si nucleus.[40,57]

$p\gamma'$) experiment. For ^{18}O and ^{19}F, we used the results of the $(\gamma, p\gamma')$ experiment.[50,44] For the ^{31}P and ^{40}Ca nuclei, the large energy of the proton hole excitation in the $1p_{1/2}$ subshell (larger than 10 MeV) makes it possible to estimate a lower bound on the probability of transitions from the outer shell using only the shape of the total cross section of the (γ, p) reaction.[55,56]

In the majority of cases, the spread in the probabilities of transitions from the outer shell is due to the uncertainty in the interpretation of the partial cross sections for population of high-lying levels of the final nuclei. All estimates refer to the region of excitation energies of the target nuclei up to 27–30 MeV.

The results given in Table IV are also shown in Fig. 9 as a function of the number of protons in the outer shell. With increasing Z, the probability of the $(2s-2d) \rightarrow (3p-3f)$ transitions increases, and in accordance with the concept of configurational splitting this is a consequence of population of the $2s-2d$ shell. Up to the ^{23}Na nucleus, which has three protons in the outer shell, the $1p \rightarrow (2s-2d)$ transitions are predominant in the photoproton channel. Beginning with ^{24}Mg, for which the number of protons in the outer shell is four, the $(2s-2d) \rightarrow (3p-3f)$ transitions are predominant in the photoproton channel.

6. COMPARISON WITH THEORETICAL STUDIES

Theoretical investigations of the process of photodisintegration of nuclei of the $2s-2d$ shell in the framework of the shell model with allowance for the residual interaction have been made for four self-conjugate nuclei: ^{20}Ne (Refs. 22 and 60), ^{24}Mg (Refs. 21, 22, 60, and 61), ^{28}Si (Refs. 22, 60, 57, 62, and 63), ^{32}S (Refs. 10, 60, 57, and 63–68). Except for the preliminary work of Ref. 21, which was made in the diagonal approximation, mixing of configurations was taken into account in all the remaining studies. Most calculations were restricted to superposition of 1p1h excitations. In Refs. 10, 60, and 67, allowance was made for the complicated structure of the ground state of the target nucleus. In the remaining cases, the ground state was chosen in the simplest form corresponding to filling of the lowest shells. Correlations in the ground state were taken into account in Refs. 60 and 61. The calculations used residual forces of zero and finite range with different amplitudes, type of mixing, and radial

TABLE V. Variants of calculations of the giant dipole resonance of nuclei of the $2s-2d$ shell (references indicated by square brackets).

Nucleus				Types of excitation		Residual forces		Ground state		
^{20}Ne	^{24}Mg	^{28}Si	^{32}S	1p1h	1p1h + more complicated	zero range	finite range	simple	complicated	correlations in the ground state
[22]	[22]	[22]	—	[22]	—	[22]	—	[22]	—	—
[60]	[60]	[60]	—	[60]	—	—	[60]	—	[60]	[60]
—	[21]	—	—	[21]	—	—	—	[21]	—	—
—	[61]	—	—	[61]	—	—	[61]	[61]	—	[61]
—	—	[62]	—	[62]	—	[62]	—	[62]	—	—
—	—	[57]	[57]	[57]	—	—	[57]	[57]	—	—
—	—	[63]	—	—	[63]	[63]	—	[63]	—	—
—	—	—	[64]	[64]	—	[64]	—	[64]	—	—
—	—	—	[65]	[65]	—	[65]	—	[65]	—	—
—	—	—	[66]	[66]	—	[66]	—	[66]	—	—
—	—	—	[67]	[67]	—	—	[67]	[67]	[67]	—
—	—	—	[68]	—	[68]	—	[68]	[68]	—	—
—	—	—	[10]	[10]	[10]	—	[10]	—	[10]	—

dependence. The theoretical investigations are briefly characterized in Table V.

We consider the details of the calculation that had a strong influence on the characteristics of the giant resonance. Analysis shows that the form of the residual forces does not have a strong influence on the energy of the dipole states or the structure of their wave functions. As a rule, the amplitude of the residual forces is chosen to reproduce the experimental position of the maximum of the giant resonance. The use of finite-range forces shifted the dipole levels compared with the calculation using zero-range forces by not more than 0.5 MeV.[62] The transition probabilities are somewhat more sensitive to the shape of the interaction, but in this case too the differences are not appreciable. Allowance for correlations in the ground state also does not lead to a significant change in the spectrum of the dipole transitions (because of the "repulsive" nature of the p–h interaction, the difference between the Tamm-Dancoff approximation and the random-phase method is small).

Other factors influencing the characteristics of the photodisintegration process are the structure of the ground state of the nucleus and configurations more complicated than 1p1h. These two factors complicate the photoabsorption spectrum without, however, leading to a significant redistribution of the gross structure of the giant resonance, and, which is particularly important, the centroids of the transitions from the different shells are situated at approximately the same energies as without allowance for these factors, and their probabilities are changed little. Figure 10 demonstrates the influence of configurations more complicated than 1p1h, but not outside the band of $1\hbar\omega$ excitations, on the characteristics of the giant dipole resonance of the ^{32}S nucleus.[10] The calculation took into account an admixture of the $2d_{3/2}$ subshell in the ^{32}S ground state. The spectrum in Fig. 10a was obtained in the 1p1h basis (12 configurations). The spectrum in Fig. 10b was obtained with allowance for the interaction of the 1p1h excitations with one- and two-phonon quadrupole vibrations of the surface. The total number of configurations participating in the calculation was 64. It can be seen that as a result of allowance for the more complicated con-

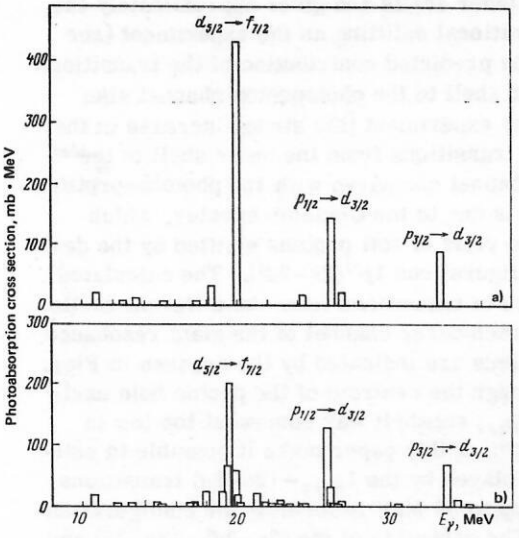

FIG. 10. Cross section for absorption of $E1$ photons by the ^{32}S nucleus.[10] a) Calculation with allowance for only 1p1h excitations; b) calculation with allowance for excitations more complicated than 1p1h.

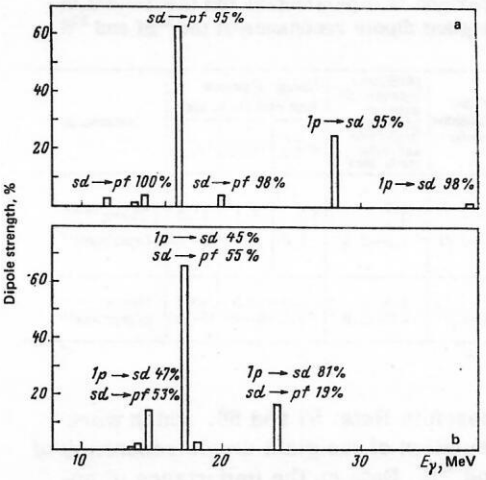

FIG. 12. Influence of the energy of the hole excitations in the $1p_{1/2}$ and $1p_{3/2}$ subshells on the characteristics of the giant dipole resonance of the ^{32}S nucleus. a) Result of calculation in accordance with Ref. 65: $E(1p_1^{-1}{}_{/2}) = 19.0$ MeV, $E(1p_3^{-1}{}_{/2}) = 28.5$ MeV; b) in accordance with Ref. 66: $E(1p_1^{-1}{}_{/2}) = 7.5$ MeV, $E(1p_3^{-1}{}_{/2}) = 13.7$ MeV.

figurations there is no significant redistribution of the dipole transitions in the giant resonance, and the gross structure of the spectrum remains.

The effects of the zeroth approximation for the energies of the single-particle transitions and, above all, the energies of the hole levels have a much greater influence on the configurational splitting and the probabilities of the transitions from the different shells. This can be clearly seen in Figs. 11 and 12. The influence of the energy of the hole excitation in the $2d_{5/2}$ subshell on the characteristics of the giant dipole resonance of the nucleus ^{32}S is demonstrated in Fig. 11.[10] The only difference between the calculations whose results are shown in this figure is the different energies of the hole

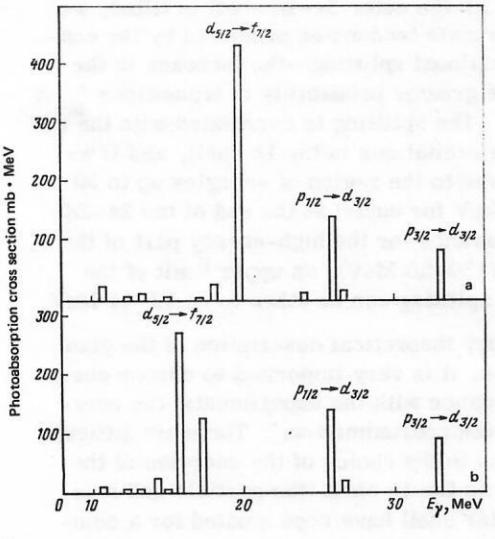

FIG. 11. Influence of energy of the hole excitation in the $2d_{5/2}$ subshell on the characteristics of the giant dipole resonance of the ^{32}S nucleus.[10] a) $E(d_5^{-1}{}_{/2}) = 7$ MeV; b) $E(d_5^{-1}{}_{/2}) = 3$ MeV.

excitation in the $2d_{5/2}$ subshell. It can be seen that a decrease in the nucleon binding energy in the $2d_{5/2}$ subshell by 4 MeV leads after diagonalization to approximately the same decrease in the energy of the $(2s-2d) \to (3p-3f)$ transitions. At the same time, the spectrum of the $1p \to (2s-2d)$ transitions is hardly changed, since in ^{32}S the $2d_{5/2}$ subshell is practically full.

The influence of the choice of the position of the holes in the $1p_{1/2}$ and $1p_{3/2}$ subsehlls on the characteristics of the giant resonance of the ^{32}S nucleus is shown in Fig. 12, in which we give the results of two calculations[65,66] made in the 1p1h approximation of the shell model and differing in the energies of the hole excitations in the $1p_{1/2}$ and $1p_{3/2}$ subshells. The fractions of the various particle–hole configurations in the wave functions of the dipole states are indicated. It can be seen that the calculation with large energies[65] of the hole excitations in the $1p$ shell (19 and 28.5 MeV for the $1p_{1/2}$ and $1p_{3/2}$ subshells) leads to strong (11–12 MeV) configurational splitting (see Fig. 12a). The calculation of Ref. 66, in which the energies of the $1p_{1/2}$ and $1p_{3/2}$ holes were taken to be much less (7.5 and 13.7 MeV, respectively), leads to mixing of the $1p \to (2s-2d)$ and $(2s-2d) \to (3p-3f)$ transitions, i.e., to an appreciable Auger effect. At the same time, the configurational splitting is reduced to 1–2 MeV (Fig. 12b).

It follows from these examples that without a correct choice of the energies of the hole excitations (especially in the $1p$ shell) it is impossible to describe satisfactorily the basic characteristics of the giant dipole resonance of nuclei of the $2s-2d$ shell. In the existing calculations, either the energy of the $1p_{3/2}^{-1}$ state was too low (if information on the zeroth approximation was taken only from pickup reactions), or the energy of the $1p_{1/2}^{-1}$ state was too high (if data on the quasielastic knockout reaction were used to determine the position of this state). The "zeroth approximation" for the $1p_{1/2}$

TABLE VI. Comparison of experimental and theoretical investigations of the giant dipole resonance of the ^{28}Si and ^{32}S nuclei.

Nucleus	Reaction	Probability of transitions from outer shell	Difference between centroids of transitions from inner and outer shells, MeV	Energy of proton hole excitation, MeV			References
				$2d_{5/2}^{-1}$	$1p_{1/2}^{-1}$	$1p_{3/2}^{-1}$	
^{28}Si	γ, tot	0.33	1.7	0	5.1	11.2	Theory[40,57]
	γ, p	0.81	2.1				
	γ, p	0.73—0.91	1.3—2.5	1.0	4.0	10—20	Experiment[40]
^{32}S	γ, tot	0.51	1.5	2.3	7.5	13.7	Theory[66]
	γ, p	0.51—1.0	1.5—2.9	4.2	8—10	15—25	Experiment[41]

hole was best chosen in Refs. 57 and 66, which were devoted to a calculation of the giant dipole resonance of the nuclei ^{28}Si and ^{32}S. Data on the importance of nucleons of different shells in the formation of the giant dipole resonance of the nuclei ^{28}Si and ^{32}S obtained from Refs. 57 and 66 are given in Table VI together with the results of experimental investigations of the photoproton decay channel of the giant resonance of these nuclei.[40,41] Such comparison is justified, since the given experimental data refer to the region up to 30 MeV, where most of the $1p_{1/2}\rightarrow(2s-2d)$ transitions are situated. In Table VI, we also compare the experimental energies of the proton hole excitations in the $2d_{5/2}$, $1p_{1/2}$, and $1p_{3/2}$ subshells with the energies used in the calculations. It can be seen that the centroid of the proton hole excitation in the $1p_{3/2}$ subshell was lowered in the calculations (especially for ^{32}S). It follows from Table VI that in the theoretical photoabsorption spectrum of the ^{28}Si nucleus transitions from the inner shell are predominant, whereas in the photoproton channel the experiments indicate that transitions from the outer shell are predominant.

On the basis of the energy eigenvalues[57] and the vectors of the dipole states in the framework of the R-matrix approach[69] a calculation was made[40] of the cross sections of the photoproton reaction with population of the levels $2d_{5/2}^{-1}$, $1p_{1/2}^{-1}$, and $1p_{3/2}^{-1}$. The theoretical cross sections for transitions from the $2d_{5/2}$ and $1p_{1/2}$ subshells are compared in Fig. 13 with the experimental data—the cross sections of the photoproton reaction corresponding to the transitions $(2s-2d)\rightarrow(3p-3f)$ and $1p_{1/2}\rightarrow(2s-2d)$. The calculation correctly reproduces the distribution of the electric dipole transitions from

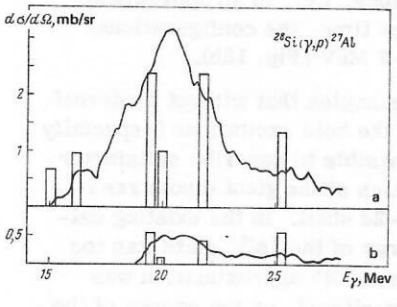

FIG. 13. Comparison of experimental[40] and theoretical[40,57] cross sections of the ^{28}Si$(\gamma,p)^{27}$Al reaction for the transitions $(2s-2d)\rightarrow(3p-3f)$ (a) and $1p_{1/2}\rightarrow(2s-2d)$ (b).

the outer and inner shells and gives approximately the same configurational splitting as the experiment (see Table VI). The predicted contribution of the transitions from the outer shell to the photoproton channel also agrees with the experiment [the strong increase in the probability of transitions from the outer shell in the photoproton channel compared with the photoabsorption cross section is due to the Coulomb barrier, which suppresses the yield of soft protons emitted by the decay of the configurations $1p^{-1}(2s-2d)$]. The calculated characteristics of transitions from the different shells in the photoproton decay channel of the giant resonance of the ^{28}Si nucleus are indicated by the crosses in Figs. 8 and 9. Although the centroid of the proton hole excitation in the $1p_{3/2}$ subshell was somewhat too low in Ref. 57, the data of this paper make it possible to estimate the part played by the $1p_{3/2}\rightarrow(2s-2d)$ transitions in the region up to 30 MeV in forming the configurational splitting. The centroids of the $(2s-2d)\rightarrow(3p-3f)$ and $1p_{1/2}\rightarrow(2s-2d)$ transitions for ^{28}Si almost coincide. Allowance for the $1p_{3/2}\rightarrow(2s-2d)$ transitions shifts the centroid of the transitions from the inner shell to energies higher by about 2 MeV. Approximately the same increase in the configurational splitting in the region below 30 MeV due to transitions from the $1p_{3/2}$ subshell is obtained from analysis of the experimental data (see Fig. 8 and Table III). Thus, correct choice of the energies of the "zeroth approximation" leads to satisfactory quantitative agreement between the theory and experiment.

7. CONCLUDING REMARKS ON THE CONFIGURATIONAL SPLITTING OF THE PHOTONUCLEAR GIANT RESONANCE

We summarize our review of configurational splitting of the photonuclear giant resonance of nuclei of the $2s-2d$ shell. As follows from the experimental data given above, configurational splitting plays an important part in forming the giant dipole resonance of nuclei of this region. As the outer $2s-2d$ shell is filled, we observe the two main tendencies predicted by the concept of configurational splitting—the increase in the splitting and the greater probability of transitions from the outer shell. The splitting is correlated with the energy of the hole excitations in the $1p$ shell, and if we restrict ourselves to the region of energies up to 30 MeV it is 6–7 MeV for nuclei at the end of the $2s-2d$ shell. With allowance for the high-energy part of the giant resonance (30–50 MeV), an upper limit of the configurational splitting can be taken to be 12–14 MeV.

For satisfactory theoretical description of the giant dipole resonance, it is very important to choose correctly (in accordance with the experiments) the energies of the "zeroth approximation." The main difficulty hitherto has been in the choice of the energies of the hole excitations in the $1p$ shell (the particle and hole levels in the outer shell have been studied for a comparatively long time and fairly reliably in single-nucleon transfer reactions). The data so far accumulated on pickup and proton quasielastic knockout reactions permit a correct choice of the energies of the hole ex-

citations in the $1p_{1/2}$ and $1p_{3/2}$ subshells. Information on a $1p_{1/2}$ subshell is provided by pickup reactions, and on the $1p_{3/2}$ subshell by quasielastic knockout of protons. The main task that now faces theory is the calculation of the characteristics of the giant dipole resonance with energies of the zeroth approximation taken from modern experimental studies. Such calculations should cover nuclei at the beginning, middle, and end of the $2s-2d$ shell, including nuclei with odd Z, for which the configurational splitting is maximal.

To describe finer details in the structure of the giant resonance and the partial decay channel, it is necessary to take into account the structure of the ground state of the nucleus and the energy spread of the particle and hole excitations. Usually, the mixing of configurations in the ground state is ignored, and the simplest form of the ground state is taken. However, mixing of configurations in the ground state is important for nuclei of the $2s-2d$ shell (see Table I). The experimental data show[40,41] that about 40 and 13% of the integrated cross section of the photoproton reaction is formed as a result of admixture of higher-lying subshells in the nuclei ^{28}Si and ^{32}S. The complicated structure of the ground state of the nucleus also leads to an enrichment of the spectrum of electric dipole excitations, improving the agreement with experiment.

Another important factor leading to a complication in the structure of the giant resonance and not taken into account in the calculations is the spread in energy of the hole excitations. It is particularly large for the $2d_{5/2}$ and $1p_{3/2}$ subshells. Thus, for the ^{32}S nucleus the proton hole excitation in the $2d_{5/2}$ subshell is distributed among eight states of the ^{31}P nucleus lying in an interval from 2.2 to 10 MeV. In the ^{27}Al nucleus, the proton hole excitation in the $2d_{5/2}$ subshell is also distributed among eight states of the ^{26}Mg nucleus lying in the interval 0–7.3 MeV. And the width of the $1p_{3/2}$ hole in the ^{28}Si nucleus is about 20 MeV. This, as we have noted above, is possibly due to the existence of many-particle excitation of $(2s-2d)^n$ configurations when the mutual orientation of the magnetic quantum numbers of the nucleons of this shell is disturbed by the "suddenly" appearing fairly large angular momentum $3/2^-$ of the deep hole. The total angular momentum of the system is $J = J_{in} + J_{hole}$. The level splitting of the $p^{-1}_{3/2}d_{5/2}$ configuration in ^{16}N–^{16}O is $\Delta V \approx 2$ MeV. Many-particle excitation will be important if the amplitudes $b \approx \Delta V/(\Delta\varepsilon - \omega)$ of the single-particle excitations are of order unity. Here, $\Delta\varepsilon \approx 10-20$ MeV is the energy spread we are discussing, and ω are the Fourier frequencies of the t-dependent external field, which must be sufficiently large in the case of stepwise "switching on" of the hole for the relation $\omega \approx \Delta\varepsilon$ to hold.

In the calculations, one can directly use data for single-nucleon transfer and quasielastic knockout reactions on the hole states and structure of the ground-state wave function of the nucleus, which to a large degree eliminates the uncertainty in these characteristics and makes it possible to determine more precisely, by comparison with experiment, the role of other factors in forming the giant resonance, such as the form and amplitude of the residual interaction and the extent to which the 1p1h excitations are coupled to more complicated excitations. However, the extent of the many-particle excitation of the $(2s-2d)^n$ configuration may be less than in the $(p, 2p)$ or $(e, e'p)$ process, since the energy $\Delta E = E\gamma \approx 25$ MeV transferred to a nucleon by a photon is appreciably less than in these processes, for which $\Delta E = E_0 - E_0' \approx 100$ MeV, i.e., the situation is more nearly adiabatic and the frequencies ω are lower.

Among the experimental tasks we can identify the following.

1. Investigation of the $1p^{-1}_{1/2}$ and $1p^{-1}_{3/2}$ states in pickup reactions for nuclei with $A > 30$. For this, it is necessary to advance into the region 10–20 MeV of excitation energies of the final nucleus.

2. Study of the partial decay channels of states lying beyond the maximum of the giant resonance, i.e., at excitation energies E_γ exceeding 30 MeV. For investigation of the possible many-particle excitations within the configuration $1p^{-1}_{3/2}(2s-2d)^{n+1}$ that we have discussed, it would be important to detect in coincidence photonucleons and comparatively soft photons [transitions between the levels of the configuration $1p^{-1}_{3/2}(2s-2d)^n$ of the nucleus $A-1$].

3. Study of the angular distributions of protons in partial transitions to the discussed hole states of the final nucleus $A-1$. Knowledge of the angular distributions will make it possible to determine the angular momentum of the emitted proton and determine directly the shell from which it came.

4. In nuclei in the middle of the $2s-2d$ shell, two-nucleon decay of the photonuclear resonance takes place with high probability. Detection in coincidence of the two nucleons with determination of their energy would make it possible to establish the energy region associated with such decay. This effect is due to decay of group B of the dipole resonance.

These are difficult problems. However, their solution will make it possible to determine more precisely the characteristics of the configurational splitting of the giant resonance of nuclei of the $2s-2d$ shell.

8. SPIN–DIPOLE TRANSITIONS IN NUCLEI OF THE 2s–2d SHELL

In dipole photoabsorption in nuclei of the $2s-2d$ shell, transitions from the closed $1p$ shell are weaker than those from the outer shell in the majority of cases. The only exceptions are the nuclei for which the number of nucleons in the valence $2s-2d$ shell is small. Moreover, by virtue of the purely dipole nature of the excitations the high-energy part of the spectrum, which is mainly associated with the transitions $1p_{3/2} \to 2d_{3/2}$, is manifested weakly (Fig. 14). The opposite picture is observed if nuclei are excited in processes which affect the spin variables of the nucleons. In the first place, this is true of backward electron scattering and muon capture. The structure of the operators responsible for the nuclear transitions in these reactions was discussed in Ref. 17. Therefore, we turn directly to the

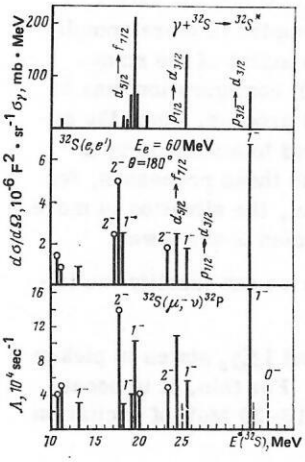

FIG. 14. Excitation spectrum (theory) of nuclear system in the case of photoabsorption,[70] inelastic backward scattering of electrons,[71] and absorption of muons[72] in the ^{32}S nucleus.

analysis of these reactions for the example of ^{32}S.

In Fig. 14 we give not only the results of theoretical analysis of excitation of the ^{32}S nucleus in dipole photoabsorption[70] but also results for backward scattering of electrons with energy $E_e = 60$ MeV (Ref. 71) and muon absorption.[72] In all three cases, the same approximation was used to describe the nuclear structure. The structure of the strongest resonances is reflected in Table VII for the example of the μ-capture process. The low-energy maximum ($E^* = 10$–15 MeV) was found to be formed by transitions of nucleons of the valence $2s$–$2d_{3/2}$ shell. Transitions of a nucleon from the $2d_{5/2}$ shell formed the peak in the region of energies from 15 to 25 MeV, and transitions from the $1p$ shell formed the peak in the high-energy region.

In both the electron scattering and the muon absorption not only states with spin $J^\pi = 1^-$ but also states with $J^\pi = 2^-$ are strongly manifested. The excitation of the latter is due to spin–dipole transitions of type $M2$. The excitation of the $J^\pi = 1^-$ levels is associated with transverse electric dipole transitions ($E1t$) in the case of electron scattering and the dipole component of the vector and axial-vector weak nucleon current in the μ-capture processes.

We consider first the excitation of states with spin $J^\pi = 1^-$. In electron scattering and in muon absorption the situation is the opposite to that in photodisintegration. The maximum of the intensity corresponds to transitions to the high-energy excitation region of the nucleus. However, as in the photonuclear reaction, the structure of the excitation spectrum is determined by configurational splitting. Moreover, it is enhanced compared with the photonuclear splitting by virtue of additional spin–orbit splitting. Such an effect also occurs in nuclei of the $1p$ shell and was discussed in detail in Ref. 17.

The magnetic quadrupole transitions of type $M2$ leading to excitation of states with spin $J^\pi = 2^-$ are localized at lower energies. But in this case too we observe configurational splitting enhanced by spin–orbit splitting.

All three results presented in Fig. 14 were obtained in the approximation of a closed $2d_{5/2}$ shell and a raised value for the position of the $1p$ hole state. If we give up the assumption that the shell is closed, and also take into account 2p2h states, whose density in the high-energy region is high, then the resonance is spread over a certain energy region. Then by the high-energy maximum shown in Fig. 14 one must understand the sum over all the states into which it is actually split. Allowance for the correction for the position of the $1p$ hole leads to a shift of the peak to lower energies.

There are hardly any experimental data on backward scattering of electrons by nuclei of the $2s$–$2d$ shell relating to the high-energy excitation region. For the ^{32}S nucleus, there are data at comparatively small angles.[73] These data, and also the results of the corresponding calculation of Ref. 10, are given in Fig. 15 (electron energy $E_e = 200$ MeV, scattering angle $\theta = 60°$). In the measured spectrum, resonances are observed in the region of high excitation energies. Unfortunately,

TABLE VII. States forming the resonance following absorption of muons by the ^{32}S nucleus and their structure.[72]

Dominant configuration	E^* (^{32}P), MeV	Transition rate	
		10^4 sec^{-1}	%
$(2s-2d_{3/2})^3 3l\,j : J = 0^-$, 1^- и 2^-	3.5—10.5	17	12
$2d_{5/2}^{-1}$ $(2s-2d_{3/2})^4 0f_{7/2}^{+}3f_{7/2} : 2^-$	10.9	13.9	10
$2d_{5/2}^{-1}$ $(2s-2d_{3/2})^4 0f_{7/2}^{+}3p_{3/2} : 1^-$	11.0	3.7	3
$(2s-2d_{3/2})^3 3f_{5/2} : 1^-$	12.5	4.2	3
$2d_{5/2}^{-1}$ $(2s-2d_{3/2})^4 0f_{7/2}^{+}3f_{7/2} : 1^-$	12.6	10.1	7
$2d_{5/2}^{-1}$ $(2s-2d_{3/2})^4 0f_{7/2}^{+}3p_{1/2} : 2^-$	13.0	4.1	3
$2d_{5/2}^{-1}$ $(2s-2d_{3/2})^4 0f_{7/2}^{+}3f_{5/2} : 2^-$	16.4	4.1	3
$2d_{5/2}^{-1}$ $(2s-2d_{3/2})^4 0f_{7/2}^{+}3f_{5/2} : 1^-$	17.5	10.9	8
$1p_{1/2}^{-1}$ $(2s-2d_{3/2})^5 : 1^-$	18.9	5.5	4
$1p_{3/2}^{-1}$ $(2s-2d_{3/2})^5 : 1^-$	26.6	15.4	11
$1p_{3/2}^{-1}$ $(2s-2d_{3/2})^5 : J$	27—29	10.5	8
All negative-parity states	—	137	100

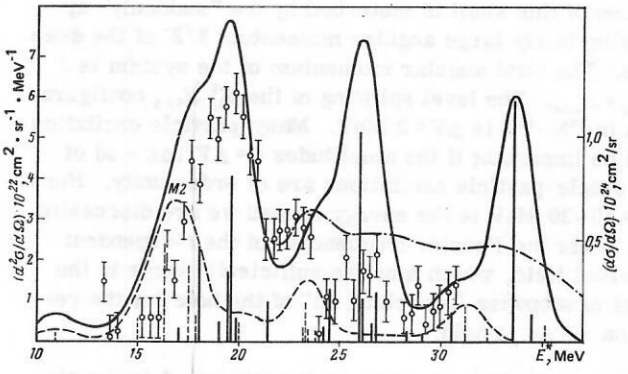

FIG. 15. Excitation spectrum of the ^{32}S nucleus in the case of inelastic scattering of electrons with energy $E_e = 200$ MeV through angle $\theta = 60.°$ The experimental data are from Ref. 73; the vertical lines are the integrated excitation cross sections of the strongest resonances[10]; the curves are obtained from the vertical lines by smearing them over an energy interval $\Gamma = 2$ MeV (continuous curve) and $\Gamma = 7$ MeV (chain curve).

the multipolarity of the corresponding transitions was not determined. The high-energy resonance was indeed found to be spread over a wide range of energies, taking a fairly large fraction of the cross section. We believe it is necessary to make a more detailed analysis of the excitation region of the nucleus from 25 to 40 MeV, not only experimentally but also theoretically. In particular, it appears important to measure the dependence of the transition form factors on the momentum transfer.

Direct observation of the excitation spectrum of a nucleus in muon absorption is unfortunately impossible. All information about the nuclear excitation is concentrated in the neutron spectrum. As will be shown below, the neutron spectra also give certain information about the high-energy peak.

The presence of a strong peak in the high-energy part of the nuclear spectrum associated with transitions of the type *Elt* is a common property of many nuclei. It can be traced[74,75] in calculations up to the nickel isotopes (Fig. 16) and will probably be manifested in even heavier nuclei. Indeed, in the case of muon absorption by the ^{88}Sr nucleus one can also, as follows from a calculation in the framework of the particle–hole approach, distinguish[76] three groups of transitions to $J^\pi T_> = 1^- 5$ states of the ^{88}Rb nucleus situated at energy 12.8 MeV: one level around 10 MeV and two in the region of 6 MeV. The excitation intensities of these levels are approximately in the ratios 5:2:1. In the first, at the highest energy, the configuration $|3f_{7/2}^{-1}4g_{7/2}\rangle$, due to excitation of a nucleon of a deeply bound shell, is predominant (with about 75% of the weight). Configurations associated with excitation of a nucleon in the $3f_{5/2}$ shell occur with large weight in the states localized in the region of excitation energy 10 MeV. The low-energy maximum is associated almost entirely with the configuration $|3p_{3/2}^{-1}4d_{5/2}\rangle$. With respect to the protons, the $3f_{5/2}$ and $3p_{3/2}$ shells in ^{88}Sr are outer shells. However, our estimate is preliminary. We need systematic

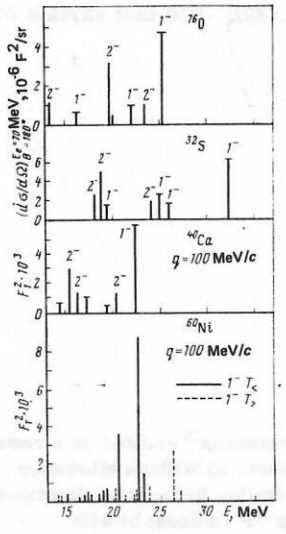

FIG. 16. Spin–dipole transitions in the nuclei ^{16}O, ^{32}S, ^{40}Ca, and ^{60}Ni in the case of electron scattering.[75]

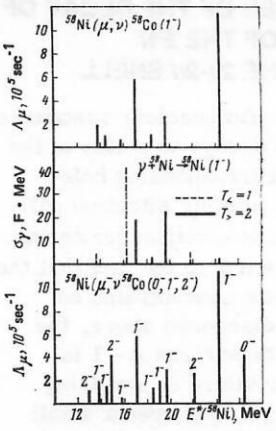

FIG. 17. Calculated excitation spectrum of the ^{58}Ni nucleus in the case of absorption of muons and γ rays.[77]

calculations taking into account the influence of complicated configurations, as was done, for example, in Ref. 75 in calculations for the nickel nuclei including phonon excitations. Nevertheless, the tendency found in the particle–hole approach for the formation of a high-energy maximum in ^{88}Sr may persist, as was the case for the nickel nuclei.

Because of isospin splitting, two high-energy peaks were found in the nickel isotopes in the nuclear excitation spectrum due to electron scattering. One, the more intense and situated in the region 20 MeV, corresponds to isospin $T = T_<$; the other, which is less intense but higher in energy, corresponds to isospin $T = T_>$. The latter forms the main maximum in the excitation spectrum of the nucleus in the case of muon absorption[77] (Fig. 17). The two peaks have the same structure, which is determined by transition of a nucleon from a deep shell.

The behavior of the form factors in the interval of excitation energies of the ^{60}Ni nucleus from 20 MeV and above with variation of the momentum transfer is such (Fig. 18) that the first level ($T_<$) is predominant up to $q \approx 140$ MeV/c, while the second ($T_>$) is more intense than all the others up to $q \approx 100$ MeV/c.[78]

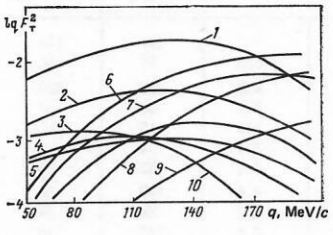

FIG. 18. Behavior of form factors of the levels in ^{60}Ni in the region of excitation energies from 20 to 32 MeV[78]: 1) $E1$ $T_<$, E = 21.73 MeV; 2) $E1$ $T_>$, E = 25.59 MeV; 3) $E2$ $T_<$, E = 24.6 MeV; 4) $E2$ $T_<$, E = 24.99 MeV; 5) $E2$ $T_<$, E = 27.14 MeV; 6) $M1$ $T_<$, E = 31.24 MeV; 7) $E2$ $T_<$, E = 28.36 MeV; 8) $M3$ $T_<$, E = 19.75 MeV; 9) $E3$ $T_<$, E = 19.96 MeV; 10) $M1$ $T_<$, E = 26.94 MeV.

9. CHARACTERISTIC FEATURES OF THE DECAY OF THE HIGH-ENERGY BRANCH OF THE $E1t$ RESONANCE IN NUCLEI OF THE $2s$-$2d$ SHELL

The high-energy branch of the photonuclear resonance due to excitation of a $1p$ nucleon decays to states of the final nucleus $A-1$ containing a corresponding hole component with large weight. A similar situation will be realized in muon absorption and electron scattering. However, there is one difference due to the fact that the greatest transition strength is now concentrated on states with a $1p_{3/2}$ hole. As we discussed above, the corresponding configuration in the nucleus $A-1$ is strongly fragmented, and its admixture in low-lying negative-parity states is not large. But even a small admixture of such configurations affects the decay of the high-energy resonance we are discussing.[79] We shall illustrate this by the example of ^{32}S.

As a result of emission of a neutron after absorption of a muon by the ^{32}S nucleus the ^{31}P nucleus is formed. The ground state and the first and third excited states of this nucleus can be described by configurations in which the $2d_{5/2}$ shell is closed.[28,80] In the second excited state ($E^*=2.2$ MeV), in contrast, the contribution of the component with a configuration containing a hole in the $2d_{5/2}$ shell is fairly large. Beginning with the eighth excited state ($E^*=4.4$ MeV), the contribution of the $2d_{5/2}$ hole component becomes decisive. The structure of all these states is reflected in Table VIII. The level at $E^*=8$ MeV can be described in two ways. In one case, it is assumed that it is described by the configuration $|0s^4 1p^{12}(2s-2d)^{n-1}(3p \text{ or } 3f)\rangle$ and does not contain an admixture of a $1p$ hole component, while in the other there is an admixture and the wave function is $\psi(E^*=8 \text{ MeV}) = |0s^4 1p^{12}(2s-2d)^{n-1}(3p \text{ or } 3f)\rangle + \alpha|0s^4 1p^{11}(2s-2d)^{n+1}\rangle$. The inclusion of the second configuration takes into account the Auger effect, when the deep hole "collapses," and the other particle is transferred to the outer shell and is emitted.

TABLE VIII. Population of ^{31}P levels as a result of decay of states forming the dipole resonance following absorption of muons by the ^{32}S nucleus (theory of Ref. 79).

Structure of states of the ^{31}P nucleus	E^* (^{31}P), MeV	Transition rate, 10^3 sec^{-1}	
		$\alpha^2=0$	$\alpha^2=0.05$
$\|(2s_{1/2}-2d_{3/2})^3: 1/2^+\rangle$	0	161	149
$\|(2s_{1/2}-2d_{3/2})^3: 3/2^+\rangle$	1.3	53	46
$\varphi_1(0_1^+: 5/2^+)$	2.2	382	320
$\|(2s_{1/2}-2d_{3/2})^3: 1/2^+\rangle$	3.1	36	33
$\|(2s_{1/2}-2d_{3/2})^3: 5/2^+\rangle$	3.3	15	12
$\|(2s_{1/2}-2d_{3/2})^3: 7/2^+\rangle$	3.4	4	2
$\|(2s_{1/2}-2d_{3/2})^3: 3/2^+\rangle$	3.5	25	21
$\varphi_1(2_1^+: J^\pi)$	4.4	199	159
$\varphi_1(0_2^+: 5/2^+)$	6.0	36	24
$\varphi_1(2_2^+: J^\pi)$	6.5	147	110
$\varphi_1(4_1^+: J^\pi)$	6.7	18	17
$\varphi_2(0_1^+: 5/2^+)$	7.0	83	33
$\sqrt{\alpha^2}\|1p^{-1}(j^1T=0)\rangle+\ldots$	8.0	—	148
$\varphi_2(2_1^+: J^\pi)$	9.2	26	15
$\varphi_2(0_2^+: 5/2^+)$	10.8	8	3
$\sqrt{\alpha^2}\|1p^{-1}(j^1T=1)\rangle$	12.0	—	48

Note. $\varphi_1(J_2^{\pi_2}\alpha: J^\pi) = \sqrt{0,30}\,|2d_{5/2}^{-1}(2s_{1/2}-2d_{3/2})^4 J_2^{\pi_2}\alpha: J^\pi\rangle+\ldots$;
$\varphi_2(J_2^{\pi_2}\alpha: J^\pi) = \sqrt{0,40}\,|2d_{5/2}^{-1}(2s_{1/2}-2d_{3/2})^4 J_2^{\pi_2}\alpha: J^\pi\rangle+\ldots$

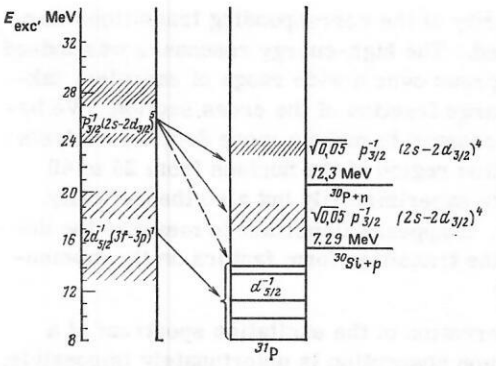

FIG. 19. Decay scheme of states of the ^{32}P nucleus formed as a result of muon absorption by the ^{32}S nucleus.

The change in the nature of the decay of the ^{32}P states formed as a result of μ capture as a function of α is reflected in Table VIII.[79] Two cases have been considered: $\alpha^2=0$, i.e., no admixture, and $\alpha^2=0.05$. Even the 5% admixture of the $1p_{3/2}$ hole configuration is sufficient for the decay of the high-energy branch of the resonance due to excitation of a $1p$ nucleon to be associated with the population of precisely these levels of the ^{31}P nucleus. The resulting decay scheme is shown in Fig. 19.

As a result of the allowance for the spread of the $1p$ hole over the states of the ^{31}P nucleus, the nature of the energy dependence of the neutron spectrum is also changed. Without allowance for the spread, the calculated spectrum is very hard, containing with high intensity neutrons with energy 15–20 MeV resulting from the decay of a high-energy resonance by virtue of an admixture of configurations containing a $2d_{5/2}$ hole to corresponding low-lying states of the ^{31}P nucleus and, in particular, to a level with $E^*=2.2$ MeV. After inclusion of the $1p_{3/2}$ hole component in the wave function of the level with energy $E^*=8$ MeV, the decay of the high-energy branch of the resonance is associated with transition to this level, and as a result the neutron spectrum becomes softer (Fig. 20). The last variant of

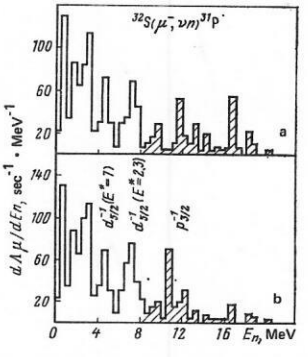

FIG. 20. Calculated spectrum of neutrons[79] emitted as a result of muon absorption by the ^{32}S nucleus. a) Without allowance for admixture of a $1p$-hole configuration in the wave functions of the negative-parity levels of the ^{31}P nucleus; b) with allowance for an admixture ($\alpha^2=5\%$). The part of the spectrum associated with decay of the high-energy branch of the resonance is hatched.

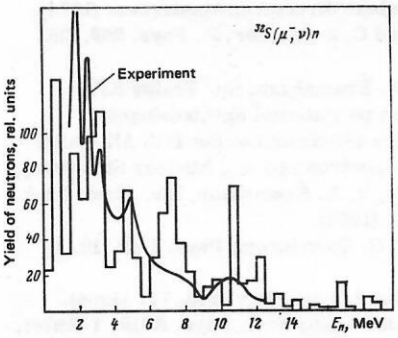

FIG. 21. Spectrum of neutrons emitted after absorption of muons by the ^{32}S nucleus. The curve is the result of the measurements of Ref. 81, and the histogram is the result of the calculation of Ref. 79 with allowance for $1p$-hole configurations in the ^{31}P nucleus.

the spectrum agrees better with the experimental one (Fig. 21)[81] and the position of the peak in the hardest part of the neutron spectrum agrees.

We now follow the fate of a state formed in the ^{31}P nucleus with negative parity. In this nucleus, the threshold for proton emission is 7.3 MeV, while that for neutron emission is 5 MeV higher. Such behavior is characteristic[23] of virtually all odd nuclei of the $2s-2d$ shell with $Z=N-1$, namely, the threshold for emission through the proton channel is in the energy interval 6–8.5 MeV, while that through the neutron channel is 4–5 MeV higher. The negative-parity levels in nuclei with $Z=N-1$ appear in the region of the proton threshold and higher. Thus, the ^{31}P nucleus formed in a negative-parity state decays subsequently through the proton channel. The proton decay will proceed by virtue of the dominant component $|1s^41p^12(2s-2d)^{n-2}(3p \text{ or } 3f)\rangle \rightarrow |1s^41p^12(2s-2d)^{n-2}\rangle$, and therefore positive-parity states are populated in the final nucleus $(A-2, Z-2)$.

We now turn to the experimental data. The lower bound on the contribution of the np channel to disintegration of the ^{24}Mg and ^{40}Ca nuclei following muon absorption is[82,83] about 5%, and for ^{28}Si it is about 10%. Moreover, it is a state of positive parity, $J^\pi=2^+$, of the ^{26}Mg nucleus that is populated with the greatest probability.[84] All this agrees well with the theoretical estimates. We note that the probability of emission of charged particles following absorption of muons is maximal for nuclei of the $2s-2d$ shell (see, for example, the review of Ref. 85). Even in nuclei of the $1p$ shell, in which the Coulomb barrier is much lower, a yield of charged particles of such intensity is not observed. It is the configurational splitting and the high excitation intensity of nucleons from the deep shell that is the reason for such an effect. Thus, the concept of configurational splitting of the dipole resonance has made it possible to describe in a uniform manner numerous effects observed in muon-absorption reactions and to relate them to one another.

Decay of states of group B in μ-capture reactions through the two-neutron channel will proceed with lower probability than through the np channel, since the energy factor in the first case is less favorable. For decay of states of group B in electroexcitation reactions a high intensity of the two-nucleon channel will also be characteristic. However, for such reactions there are as yet no measurements. In photonuclear reactions, as follows from the data given earlier, the following picture is observed: in ^{24}Mg the contribution of the $(\gamma, 2p)$ channel is about 10%, and in ^{32}S it is about 20%. For the ^{26}Mg and ^{28}Si nuclei, the contribution of the two-nucleon channels [respectively, (γ, np) and $(\gamma, 2p)$] is small, apparently less than 1%.

CONCLUSIONS

In this and the earlier review of Ref. 17, we have considered many questions related to the excitation and subsequent decay of states of the giant dipole resonance in light nuclei and nuclei of medium mass. The particles exciting the nuclei are very varied: γ rays, electrons, muons, π and K mesons. The interactions due to these particles are purely electromagnetic, strong in conjunction with electromagnetic, and weak. However, irrespective of the particle species and the interaction, the response of the nuclear system has been found to be universal and to consist of excitation of states of the giant-resonance type, these exhibiting very varied degrees of collectivization. The universality of the response of the nuclei, i.e., the fact that it is independent of the particular type of disturbance (at least in the considered processes), is due to the circumstance that only the tensor structure of the disturbance determines the type of the resonance that can be excited in the considered reactions. The momenta transferred to the nuclear system were chosen to ensure that the dipole and spin–dipole resonances are everywhere dominant.

On the basis of the analysis of the results of the experimental and theoretical investigations we have established and analyzed a universal property of the dipole resonance in light and medium nuclei—configurational splitting. The concept of configurational splitting has made it possible to unify a large number of phenomena that occur in the excitation and decay of the states that form the dipole resonance and to explain them from a common point of view. Much attention in this and the earlier review[17] has been paid to hitherto little studied specific features of the nuclear structure due to the configurational splitting. In nuclei of the $1p$ shell these are various types of star decay of excited states with different multiplet structures and the gradual transition to a quasi-α-particle mechanism of absorption of γ rays with increasing energy of the latter. Intimately related to this question is the new problem of the decay of Λ hypernuclei of the $1p$ shell. In nuclei of the $2s-2d$ shell, we are concerned with the position and energy spread for the $1p$ holes. The data of the photonuclear reactions agree on the whole with the assumption that only the $(p, 2p)$ and $(e, e'p)$ processes actually affect the $1p_{3/2}$ holes, in contrast to the $(d, ^3\text{He})$ processes. But for a fuller elucidation of this question it is necessary to investigate the giant resonance in the energy range 30–40 MeV, to say nothing of $(p, 2p)$ and $(e, e'p)$ processes with high resolution. For the theory of photonuclear reactions, an important question here is that of

the microscopic description of the spreading of very broad $1p$ hole levels ($\Gamma \approx 10-20$ MeV).

Finally, the (e,e') and (π,γ) processes and μ capture make it possible to use the spin–orbit splitting to obtain, even in nuclei with closed shells and nuclei of medium mass, isolated high-lying single-particle particle–hole components (with a hole in a closed shell) embedded in a continuum of states of statistical type. These are also undoubtedly objects of great interest for investigation, especially from the point of view of their decay. In attracting attention to these questions, we hope that they will stimulate the interest of the experimentalists. We can then hope to obtain answers to the open questions found and posed in the discussion of the configurational splitting of the dipole resonance.

[1]D. H. Wilkinson, Physica (Utrecht) **22**, 1039 (1956).
[2]G. E. Brown and M. Bolsterli, Phys. Rev. Lett. **3**, 472 (1959).
[3]J. P. Elliot and B. H. Flowers, Proc. R. Soc. London Ser. A **242**, 57 (1957); V. V. Balashov, V. G. Shevchenko, and N. P. Yudin, Zh. Eksp. Teor. Fiz. **41**, 1929 (1961) [Sov. Phys. JETP **14**, 1371 (1962)]; G. E. Brown, L. Castillejo, and J. A. Evans, Nucl. Phys. **22**, 1 (1961).
[4]G. E. Brown, J. A. Evans, and D. J. Thouless, Nucl. Phys. **24**, 1 (1961); N. Vinh-Mau and G. E. Brown, Nucl. Phys. **29**, 89 (1962); A. M. Lane, Nuclear Theory: Pairing Force Correlation and Collective Motion, Benjamin, New York (1964) [Russian translation published by Atomizdat, Moscow (1967)].
[5]A. B. Migdal, Teoriya konechnykh fermi-sistem i svoĭstva atomnykh yader, Nauka, Moscow (1965); English translation: Theory of Finite Fermi Systems, Interscience, New York (1967).
[6]A. B. Migdal, Zh. Eksp. Teor. Fiz. **15**, 81 (1945).
[7]M. Danos, Nucl. Phys. **5**, 23 (1958); K. Okamoto, Phys. Rev. **110**, 143 (1958).
[8]H. Morinaga, Z. Phys. **188**, 182 (1965); S. Fallieros, B. F. Goulard, and R. H. Venter, Phys. Lett. **19**, 398 (1965); V. V. Balashov and E. L. Yadrovsky, Phys. Lett. **22**, 507 (1966).
[9]H. J. Weber, M. G. Huber, and W. Greiner, Z. Phys. **192**, 223 (1966).
[10]L. Majling *et al.*, Nucl. Phys. **A143**, 429 (1970); M. A. Zhusupov, V. V. Karapetyan, and R. A. Éramzhyan, Izv. Akad. Nauk SSSR, Ser. Fiz. **33**, 730 (1969).
[11]V. V. Balashov and V. M. Chernov, Zh. Eksp. Teor. Fiz. **43**, 227 (1962) [Sov. Phys. JETP **16**, 162 (1963)]; V. V. Balashov, Nucl. Phys. **40**, 93 (1963); M. Danos and W. Greiner, Phys. Rev. **138**, B876 (1965); V. Gillet, M. A. Melkanoff, and J. Raynal, Nucl. Phys. **A97**, 631 (1967).
[12]F. E. Bertrand, Nucl. Phys. **A354**, 129 (1981).
[13]L. S. Cardman, Nucl. Phys. **A354**, 173 (1981).
[14]V. G. Neudachin, V. G. Shevchenko, and N. P. Yudin, in: Trudy tret'eĭ Vsesoyuznoĭ konferentsii po yadernym reaktsiyam pri malykh i srednikh énergiyakh, 1960 (Proc. of the Third All-Union Conf. on Nuclear Reactions at Low and Medium Energies), USSR Academy of Sciences, Moscow–Leningrad (1962), p. 495; V. G. Neudatchin and V. N. Orlin, Nucl. Phys. **31**, 338 (1962); V. G. Neudatchin, V. G. Shevchenko, and N. P. Yudin, Phys. Lett. **10**, 180 (1964).
[15]V. G. Neudachin and Yu. F. Smirnov, Nuklonnye assotsiatsii v legkikh yadrakh (Nucleon Associations in Light Nuclei), Nauka, Moscow (1969).
[16]F. C. Barker *et al.*, Nucl. Phys. **28**, 96 (1961); Nucl. Phys. **45**, 443 (1963).
[17]B. S. Ishkhanov *et al.*, Fiz. Elem. Chastits At. Yadra **12**, 905 (1981) [Sov. J. Part. Nucl. **12**, 362 (1981)].
[18]G. Jacob and Th. A. J. Maris, Rev. Mod. Phys. **45**, 6 (1973); Th. A. J. Maris, in: Proc. of the Fifth Intern. Conf. on High Energy Physics and Nuclear Structure, Amsterdam (1974).
[19]H. Mackh, G. Mairle, and C. J. Wagner, Z. Phys. **269**, 353 (1974).
[20]V. V. Balashov and R. A. Éramzhyan, in: Tezisy XIV Vsesoyuz. soveshchaniya po yadernoĭ spektroskopii i strukture atomnogo yadra (Abstracts of the 14th All-Union Symposium on Nuclear Spectroscopy and Nuclear Structure), Nauka, Leningrad (1963); R. A. Éramzhyan, Izv. Akad. Nauk SSSR, Ser. Fiz. **28**, 1181 (1964).
[21]V. G. Neudatchin and V. G. Shevchenko, Phys. Lett. **12**, 18 (1964).
[22]W. Bassichis and F. Scheck, Phys. Rev. **145**, 771 (1966).
[23]P. M. Endt and C. Van der Leun, Nucl. Phys. **A310**, 1 (1978); F. Ajzenberg-Selove, Nucl. Phys. **A281**, 1 (1977); **A300**, 1 (1978).
[24]B. Castel, I. P. Johnstone, and B. P. Singh, Nucl. Phys. **A157**, 137 (1970).
[25]M. Blann, Ann. Rev. Nucl. Sci. **25**, 123 (1975); K. Seidel *et al.*, Fiz. Elem. Chastits At. Yadra **7**, 499 (1976) [Sov. J. Part. Nucl. **7**, 192 (1976)].
[26]J. Mougey *et al.*, Nucl. Phys. **A262**, 461 (1976).
[27]H. E. Gove *et al.*, Nucl. Phys. **A116**, 369 (1968).
[28]B. H. Wildenthal and E. Newman, Phys. Rev. **167**, 1027 (1968).
[29]R. E. Tribble and K. I. Kubo, Nucl. Phys. **A282**, 269 (1977).
[30]J. D. Sherman *et al.*, Nucl. Phys. **A257**, 45 (1976).
[31]E. Gerlic *et al.*, Phys. Rev. C **12**, 2106 (1975).
[32]W. Fritsch, R. Lipperheide, and U. Willie, Nucl. Phys. **A198**, 515 (1972); A. Faessler, S. Kusuno, and G. L. Strobel, Nucl. Phys. **A203**, 513 (1973); P. Nozières and S. T. De Dominicis, Phys. Rev. **178**, 1097 (1969).
[33]P. M. Endt, At. Data Nucl. Data Tables **19**, 23 (1977).
[34]R. P. Singhal *et al.*, Nucl. Phys. **A323**, 91 (1979).
[35]B. H. Wildenthal *et al.*, Phys. Rev. C **4**, 1708 (1971).
[36]B. S. Ishkhanov *et al.*, Yad. Fiz. **33**, 865 (1981) [Sov. J. Nucl. Phys. **33**, 453 (1981)].
[37]B. S. Ishkhanov *et al.*, Yad. Fiz. **33**, 581 (1981) [Sov. J. Nucl. Phys. **33**, 303 (1981)].
[38]V. V. Varlamov *et al.*, Yad. Fiz. **30**, 1185 (1979) [Sov. J. Nucl. Phys. **30**, 617 (1979)].
[39]B. S. Ishkhanov *et al.*, Nucl. Phys. **A313**, 317 (1979).
[40]V. V. Varlamov *et al.*, Izv. Akad. Nauk SSSR, Ser. Fiz. **43**, 186 (1979).
[41]V. V. Varlamov *et al.*, Yad. Fiz. **28**, 590 (1978) [Sov. J. Nucl. Phys. **28**, 302 (1978)].
[42]J. T. Caldwell, S. C. Fultz, and R. L. Bramblett, Phys. Rev. Lett. **19**, 447 (1967).
[43]Y. S. Horowitz *et al.*, Nucl. Phys. **A151**, 161 (1970).
[44]J. E. M. Thomson and M. N. Thompson, Nucl. Phys. **A330**, 66 (1979).
[45]B. S. Ishkhanov *et al.*, Yad. Fiz. **32**, 885 (1980) [Sov. J. Nucl. Phys. **32**, 455 (1980)].
[46]K. Bangert *et al.*, Nucl. Phys. **A261**, 149 (1976).
[47]J. E. M. Thomson and M. N. Thompson, Nucl. Phys. **A285**, 84 (1977).
[48]J. E. M. Thomson, M. N. Thompson, and R. J. Stewart, Nucl. Phys. **A290**, 14 (1977).
[49]D. Brajnik *et al.*, in: Proc. of the Fifth Intern. Betatron Symposium, Bucharest (1971), p. 217.
[50]K. Bangert *et al.*, Z. Phys. **A278**, 295 (1976).
[51]B. H. Wildenthal and E. Newman, Phys. Rev. **175**, 1431 (1968).
[52]M. Arditi *et al.*, Nucl. Phys. **A165**, 129 (1971).
[53]C. I. Wagner *et al.*, Nucl. Phys. **A125**, 80 (1969).
[54]F. P. Brady *et al.*, Nucl. Phys. **A288**, 269 (1977).
[55]B. S. Ishkhanov *et al.*, Phys. Lett. **9**, 1901 (1974).
[56]D. Brajnik *et al.*, Phys. Rev. **9**, 1901 (1974).
[57]S. A. Farris and J. M. Eisenberg, Nucl. Phys. **88**, 241 (1966).
[58]J. Ahrens *et al.*, in: Proc. of the Intern. Conf. on Photonuclear Reactions and Applications, Asilomar (1973), p. 23.
[59]R. Ö. Akyüz and S. Fallieros, Phys. Rev. Lett. **27**, 1016 (1971).

[60]S. S. M. Wong, D. J. Rowe, and J. C. Parikh, Phys. Lett. **48B**, 403 (1974).
[61]S. G. Nilsson, J. Sawicki, and N. K. Glendenning, Nucl. Phys. **33**, 239 (1961).
[62]L. N. Bolen and J. M. Eisenberg, Phys. Lett. **9**, 52 (1964).
[63]D. Drechsel, J. B. Seaborn, and W. Greiner, Phys. Rev. **162**, 983 (1967).
[64]B. M. Spicer, Aust. J. Phys. **18**, 1 (1966).
[65]H. Lichtblau and B. M. Spicer, Aust. J. Phys. **19**, 297 (1966).
[66]L. L. Hill and H. Überall, Phys. Lett. **B24**, 364 (1967).
[67]B. I. Goryachev *et al.*, Nucl. Phys. **A93**, 232 (1967).
[68]D. V. Webb, B. M. Spicer, and H. Arenhövel, Phys. Rev. **164**, 1397 (1967).
[69]A. M. Lane, Rev. Mod. Phys. **32**, 519 (1960).
[70]Yu. I. Bely *et al.*, Nucl. Phys. **A170**, 141 (1971).
[71]Yu. I. Belyĭ and N. M. Kabachnik, Yad. Fiz. **14**, 1113 (1971) [Sov. J. Nucl. Phys. **14**, 619 (1972)].
[72]Yu. I. Bely *et al.*, Nucl. Phys. **A204**, 357 (1973).
[73]I. S. Gul'karov *et al.*, Yad. Fiz. **10**, 694 (1969) [Sov. J. Nucl. Phys. **10**, 400 (1970)].
[74]R. A. Eramzhyan, L. Majling, and J. Rizek, Czech. J. Phys. **31**, 482 (1981).
[75]N. G. Goncharova and R. A. Eramzhyan, Z. Phys. **A306**, 89 (1982).
[76]J. Joseph, F. Ledoyen, and B. Goulard, Phys. Rev. C **6**, 1742 (1972).
[77]O. Nalcioglu, D. J. Rowe, and C. Ngo-Trong, Nucl. Phys. **A218**, 495 (1974).
[78]N. G. Goncharova, G. Mishchenko, and R. A. Éramzhyan, Izv. Akad. Nauk SSSR, Ser. Fiz. **46**, 2111, 2117 (1982).
[79]R. A. Eramzhyan, L. Majling, and J. Rizek, Nucl. Phys. **A247**, 411 (1973).
[80]P. W. M. Glaudemans, G. Wiechers, and P. J. Brussard, Nucl. Phys. **56**, 529, 548 (1964).
[81]V. Evseev *et al.*, Phys. Lett. **B28**, 553 (1969); in: High Energy Physics and Nuclear Structure, Plenum Press, New York (1970), p. 157.
[82]T. Pratt, Nuovo Cimento **B61**, 119 (1969).
[83]P. Igo-Kemenes *et al.*, Phys. Lett. **34**, 286 (1971).
[84]G. H. Miller *et al.*, Phys. Rev. C **6**, 487 (1972).
[85]Yu. A. Batusov and R. A. Éramzhyan, Fiz. Elem. Chastits At. Yadra **8**, 229 (1977) [Sov. J. Part. Nucl. **8**, 95 (1977)].

Translated by Julian B. Barbour